*Graphical Abstract

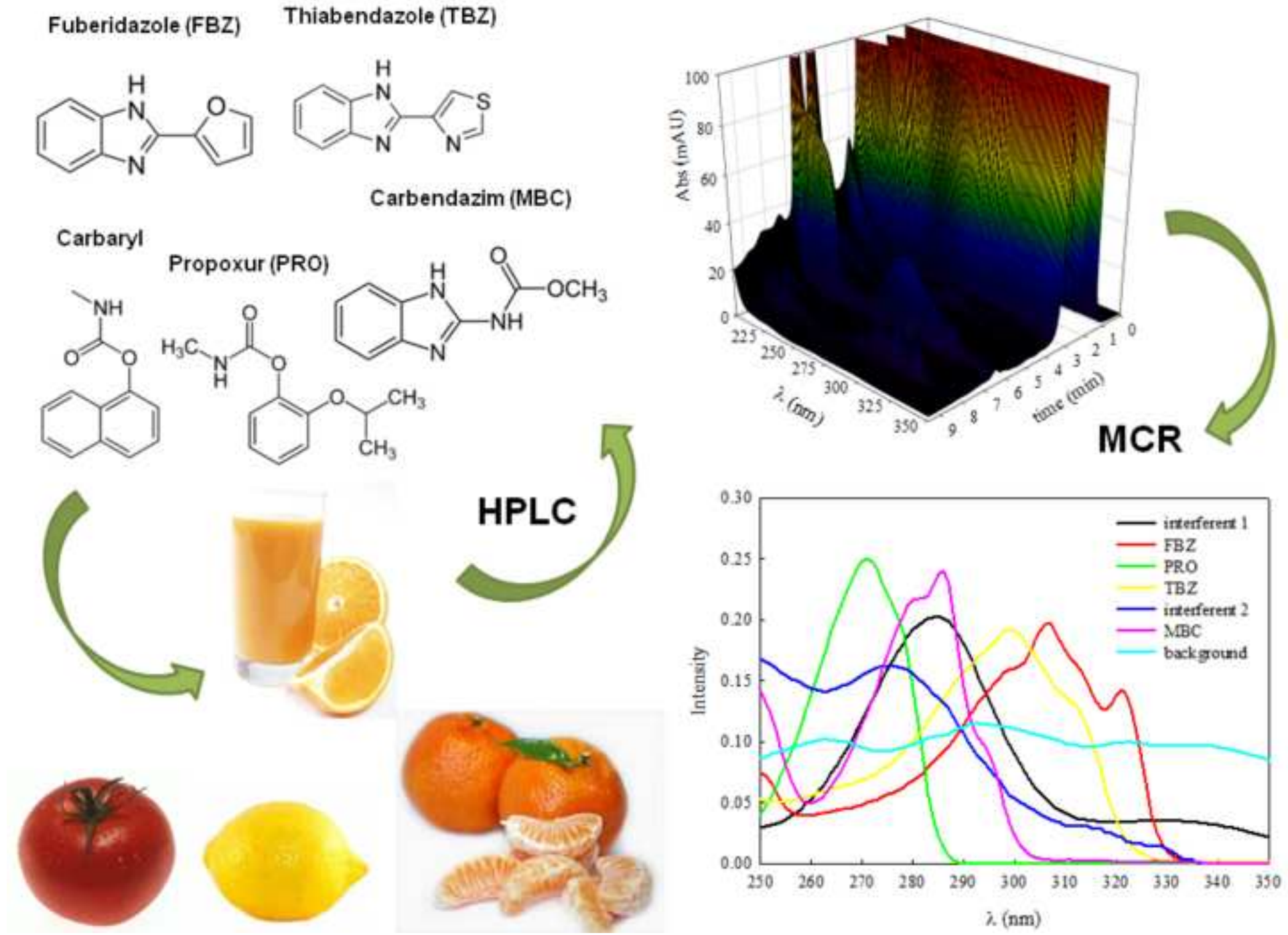

***Highlights**

- Five pesticides were determinted in juice, fruit and vegetable samples
- Liquid chromatography was coupled to diode array detection
- Chromatographic-spectral matrices were analyzed by multivariate curve resolution

Determination of five pesticides in juice, fruit and vegetable samples by means of liquid chromatography combined with multivariate curve resolution

Valeria Boeris, Juan A. Arancibia, Alejandro C. Olivieri

Departamento de Química Analítica, Facultad de Ciencias Bioquímicas y Farmacéuticas, Universidad Nacional de Rosario e Instituto de Química Rosario (IQUIR-CONICET), Suipacha 531(S2002LRK) Rosario, Argentina.

Corresponding author:

Alejandro Olivieri

Tel./fax: +54 3414372704.

E-mail addresses: olivieri@iquir-conicet.gov.ar, aolivier@fbioyf.unr.edu.ar

Abstract

The aim of this work was to quantify five commonly used pesticides (propoxur, carbaryl, carbendazim, thiabendazole and fuberidazole) in real samples as: tomato, orange juice, grapefruit juice, lemon and tangerine. The method used for the determination of these analytes in the complex matrices was high-performance liquid chromatography with diode array detection. In order to work under isocratic conditions and to complete each run in less than 10 min, the analysis was carried out applying multivariate curve resolution coupled to alternating least-squares (MCR–ALS). The flexibility of this applied multivariate model allowed the prediction of the concentrations of the five analytes in complex samples including strongly coeluting analytes, elution time shifts, band shape changes and presence of uncalibrated interferents. The obtained limits of detection (in $\mu g\ L^{-1}$) using the proposed methodology were 2.3 (carbendazim), 0.90 (thiabendazole), 12 (propoxur), 0.46 (fuberidazole) and 0.32 (carbaryl).

Keywords

High-performance liquid chromatography; Diode array detection; Multivariate curve resolution; Pesticides; Vegetable samples

Abbreviations

High-performance liquid chromatography (HPLC), diode array detection (DAD), multivariate curve resolution coupled to alternating least-squares (MCR-ALS),

propoxur (PRO), carbaryl (CBL), carbendazim (MBC), thiabendazole (TBZ), fuberidazole (FBZ)

1. Introduction

Although the use of pesticides provides unquestionable benefits in providing a plentiful, low-cost supply of high-quality fruits and vegetables, their incorrect application may leave harmful residues, which involve possible health risk [1]. The concentration of pesticides is regulated in many samples such as drinking waters, vegetables, juices, etc., by the European Commission [2] and the Food and Drug Administration [3], among other agencies. Traditionally, the instrumental techniques employed to determine these compounds involve fluorescence, gas or liquid chromatography [4-8]. Specifically, the determination of benzimidazolic pesticides (carbendazim, thiabendazole and fuberidazole) and/or carbamates (carbaryl, propoxur and carbendazim) in fruits and vegetables have been carried out by various approaches, such as supramolecular solvent-based microextraction followed by high-performance liquid chromatography (HPLC) with fluorescence detection [9], gas chromatography coupled to mass spectrometry and selected ion monitoring [10], enzymatic immunoassay using antibodies [11-13] or electrochemical methods [14, 15].

The analysis of mixtures of pesticides using methods based on HPLC sometimes results in complex separations and overlapped peaks [16, 17]. Nevertheless, complex multicomponent mixtures can in many cases be qualitatively and quantitatively resolved by means of chemometrics. Depending on their nature, data can be arranged in a two-way structure (a table or a matrix), as in

60 the case of collecting the absorbance spectra for many samples, or in a three-way
61 structure, e.g. in HPLC with diode array detection (DAD), where spectra are
62 recorded at several elution times for each sample. Such data arrangements in
63 three- or higher way arrays can be handled using multi-way methods of analysis
64 [18, 19].

65 Collection of multi-dimensional chromatographic information, and data
66 processing by advanced chemometric algorithms constitute a fruitful combination
67 of techniques, recently applied to diverse research areas [20-22]. Chemometrics is
68 required whenever perfect separation of the various sample components cannot be
69 achieved by the employed chromatographic system, leading to overlapping peaks
70 in the elution time mode. In these cases, selectivity may be mathematically
71 restored by applying multivariate data analysis [23]. In particular, the so-called
72 second-order advantage can be achieved, a property which is inherent to matrix
73 instrumental data, and implies that analytes can be quantified in samples
74 containing potential interferences [21]. Signals arising from coeluting analytes or
75 foreign components can be modeled by powerful second-order multivariate
76 algorithms.

77 The combination of chemometrics to HPLC presents additional advantages
78 in relation to traditional methods: since chemometrics allows resolving coeluted
79 peaks, it is possible to reduce the duration of the chromatographic run, allowing not
80 only processing more samples but also reducing the solvent consumption, saving
81 time and money. Moreover, several authors report that gradient of solvents was
82 required to achieve resolution of the analytes [24-26]: this requirement may be

avoided using isocratic conditions and resolving the peak by applying chemometrics.

In liquid chromatographic runs, elution time shifts and band shape changes usually occur from sample to sample: in these cases, a useful alternative is to analyze the data with flexible algorithms, which allow a given component to present different time profiles in different samples, such as parallel factor analysis 2 (PARAFAC2) or multivariate curve resolution coupled to alternating least-squares (MCR-ALS) [27]. Recent work from our laboratory indicated better performance with MCR–ALS in the case of multi-analyte quantification in the presence of high overlapping of elution profiles and uncalibrated interferences, mainly because of the possibility of building a more constrained model in MCR–ALS in comparison with PARAFAC2 [22].

In the present report, we selected MCR–ALS as the algorithm of choice for processing HPLC-DAD data, and discuss its behavior towards the quantification of the following five pesticides in fruit and vegetable samples: propoxur (PRO), carbaryl (CBL), carbendazim (MBC), thiabendazole (TBZ) and fuberidazole (FBZ) (Fig. 1). The presence of benzimidazoles, carbamates and their degradation products in waters or food products is potentially harmful for humans due to their proven toxicity. This is the cause of the continued interest in the development of analytical methods for monitoring these families of compounds. Previous chromatographic analysis of the presently studied compounds required up to 35 min [28, 29]. The aim of this work is to quantify these analytes in complex matrices under HPLC isocratic conditions and in less than 10 min.

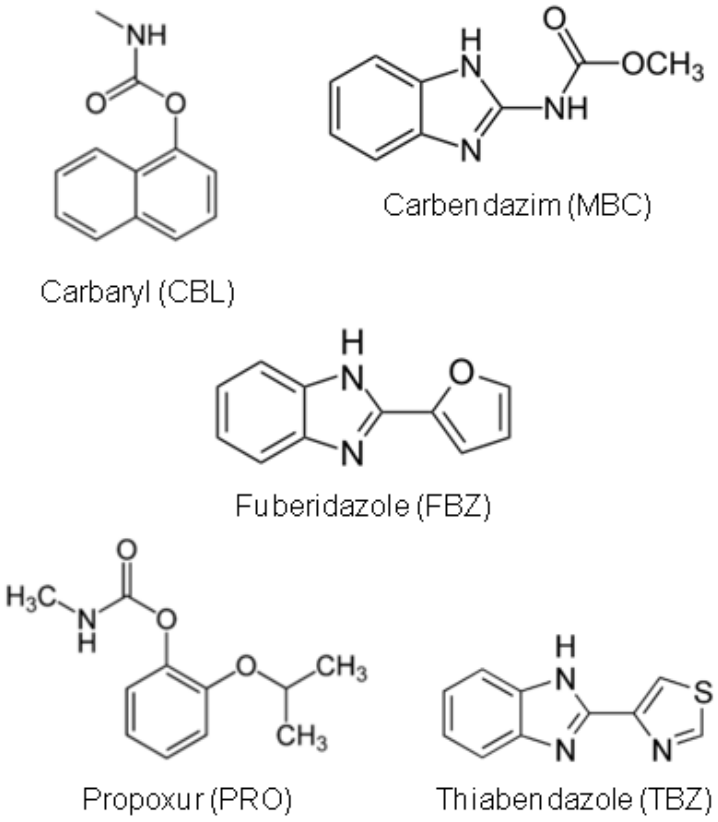

Figure 1

2. Theory

The bilinear model assumed by MCR methods is analogous to the generalized Lambert-Beer's law, where the individual responses of each component are additive. In matrix form, this bilinear model is expressed as:

$$\mathbf{D} = \mathbf{C}\,\mathbf{S}^{T} + \mathbf{E} \quad (1)$$

where **D** (size $J \times K$) is the matrix of experimental data (J is the number of elution time data points and K is the number of absorption wavelengths), **C** (size $J \times N$) is the matrix whose columns contain the concentration profiles of the N components present in the samples, $\mathbf{S}^{T}$ (size $N \times K$) is the matrix whose rows contain the

component spectra and **E** (size $J \times K$) is a matrix collecting the experimental error and the variance not explained by the bilinear model of equation (1).

The first step in MCR-ALS studies is to obtain a rough estimation of the number of components, which can be simply performed by visual inspection of singular values or principal component analysis (PCA) [30, 31].

The resolution is accomplished using an iterative ALS procedure, initialized using an initial estimation of the spectral or concentration profiles for each intervening species. Different methods are used for this purpose, such as evolving factor analysis [32] or the determination of the purest variables [33]. If the initial estimations are the spectral profiles, the unconstrained least-squares solution for the concentration profiles can be calculated from the expression:

$$\mathbf{C} = \mathbf{D}\,(\mathbf{S}^{T})^{+} \qquad (2)$$

where $(\mathbf{S}^{T})^{+}$ is the pseudoinverse of the spectral matrix $\mathbf{S}^{T}$ [34]. If the initial estimations were the concentration profiles, the unconstrained least-squares solution for the spectra can be calculated from the expression:

$$\mathbf{S}^{T} = \mathbf{C}^{+}\,\mathbf{D} \qquad (3)$$

where $\mathbf{C}^{+}$ is the pseudoinverse of **C**. Both steps can be implemented in an alternating least-squares cycle, so that, at each iteration, new **C** and $\mathbf{S}^{T}$ matrices are obtained. During these iterative recalculations of **C** and $\mathbf{S}^{T}$**,** a series of constraints (e.g. non-negativity, unimodality and sample selectivity; the latter removes a component which is known to be absent in a given sample) could be applied to give physical meaning to the obtained solutions, and to limit their possible number for the same data fitting and decrease the extent of possible

rotation ambiguities [35]. Iterations continue until an optimal solution is obtained that fulfils the postulated constraints and the established convergence criteria.

The procedure described above can be easily extended to the simultaneous analysis of multiple data sets or data matrices if they have at least one data mode (direction) in common. For instance, if the different data sets have been analyzed by the same spectroscopic method, the possible data arrangement and bilinear model extension is given by the following equation:

$$\mathbf{D}_{\mathbf{aug}} = \begin{bmatrix} \mathbf{D}_{\mathbf{cal1}} \\ \mathbf{D}_{\mathbf{cal2}} \\ \cdots \\ \mathbf{D}_{\mathbf{test}} \end{bmatrix} = \begin{bmatrix} \mathbf{C}_{\mathbf{cal1}} \\ \mathbf{C}_{\mathbf{cal2}} \\ \cdots \\ \mathbf{C}_{\mathbf{test}} \end{bmatrix} \mathbf{S}^{\mathbf{T}} + \begin{bmatrix} \mathbf{E}_{\mathbf{cal1}} \\ \mathbf{E}_{\mathbf{cal2}} \\ \cdots \\ \mathbf{E}_{\mathbf{test}} \end{bmatrix} = \mathbf{C}_{\mathbf{aug}} \mathbf{S}^{\mathbf{T}} + \mathbf{E}_{\mathbf{aug}} \tag{4}$$

where $\mathbf{D}_{aug}$ is the augmented data matrix, constructed from I individual data matrices [36], corresponding to the set of calibration samples ($\mathbf{D}_{cal1}$, $\mathbf{D}_{cal2}$, ...) and to a single test sample ($\mathbf{D}_{test}$).

In this case, $\mathbf{C}_{aug}$ is the column-wise augmented matrix of concentration profiles (size $JI \times N$, where N is the number of responsive chemical components), $\mathbf{S}^{T}$ is the matrix of loadings (dimensions $N \times K$) in the row vector space, and $\mathbf{E}_{aug}$ collects the residuals. After decomposition, the scores for analyte n are computed as the sum of the elements of the corresponding profile in each of the sub-matrices of $\mathbf{C}_{aug}$.

Finally, the calibration scores are employed to build a pseudo-univariate calibration line, leading to an estimation of the corresponding slope (m_n) and offset (n_n). The analyte score in the test sample is then interpolated in the calibration line to yield the predicted analyte concentration c_n:

$$c_n = (a_{test,n} - n_n) / m_n \quad (5)$$

3. Experimental

3.1. Reagents

Carbendazim (MBC), thiabendazole (TBZ), fuberidazole (FBZ), propoxur (PRO) and carbaryl (CBL) were purchased from Sigma Aldrich Co. (St. Louis, MO). Methanol was obtained from Merck. Milli-Q water (Millipore) was used in all experiments. Solvents were filtered through 0.45 µm filters.

3.2. Stock standard and working standard solutions

Stock standard solutions of MBC (570 mg L^{-1}), TBZ (1150 mg L^{-1}), FBZ (620 mg L^{-1}), PRO (1720 mg L^{-1}) and CBL (680 mg L^{-1}) were prepared in 25.00 mL volumetric flasks by dissolving accurately weighed amounts of the drugs in methanol and completing to the mark with the same solvent. From these solutions, more diluted solutions were obtained (MBC 22.8 mg L^{-1}, TBZ 20.7 mg L^{-1}, FBZ 9.92 mg L^{-1}, PRO 172 mg L^{-1}, CBL 13.6 mg L^{-1}). Working solutions were prepared immediately before their use by taking appropriate aliquots of solutions and diluting with methanol and water (50:50 v/v) to the desired concentrations.

3.3. Apparatus

Chromatographic runs were performed on an HP 1200 liquid chromatograph (Agilent Technologies, Waldbronn, Germany) consisting of a quaternary pump, a manual injector fitted with a 200 µL loop and a diode array UV–visible detector set at a wavelength range from 200 to 350 nm. A C18 column of 150mm×4.6mm, 5µm

185 particle size was employed (Agilent Sorbax SB). The data were collected using the
186 software HP ChemStation for LC Rev.HP 1990–1997.
187
188 **3.4. Software**
189 The data were handled using the MATLAB computer environment [37]. The
190 calculations involved in the mixture resolution by MCR-ALS have been made using
191 mvc2_gui, a MATLAB graphical interface toolbox which is a new version of that
192 already reported in the literature [38].
193
194 **3.5. Calibration and validation samples**
195 In order to design the calibration set, preliminary experiments were
196 performed with the pure analytes, showing that the full elution time range could be
197 divided into three relevant regions: an overlapped zone where three analytes
198 appear (TBZ, PRO and FBZ) and two regions where the remaining two analytes
199 are fully resolved (MBC and CRL). A set of 18 calibration solutions containing the
200 analytes in the ranges 0 - 228 $\mu g\ L^{-1}$ for MBC, 0 - 207 $\mu g\ L^{-1}$ for TBZ, 0 - 1720 $\mu g\ L^{-1}$ for PRO, 0 – 99.2 $\mu g\ L^{-1}$ for FBZ and 0 - 136 $\mu g\ L^{-1}$ for CBL were prepared in
202 appropriate volumetric flasks. The concentrations are collected in Table 1. Fifteen
203 of these samples correspond to the concentrations provided by a central composite
204 design for the three analytes appearing in the overlapped region: TBZ, PRO and
205 FBZ. Each of the remaining three samples of the 18-sample set corresponds to
206 each of the three pure analytes at their maximum levels. Each of these 18 samples
207 was combined with nine equally spaced, duplicate concentration levels for the two

208 resolved analytes. For establishing the calibration concentration ranges, the linear
209 range for all components was studied by analyzing different solutions covering the
210 interval 0–2000 μg L^{-1}.

211 A validation set of 10 samples was also prepared, containing the five
212 analytes in concentrations different than those used for calibration, and following a
213 random design, i.e., the specific concentrations were taken as random numbers
214 generated within the calibration domain.

215

216 **3.6. Samples and sample preparation**

217 Tangerine, lemon, tomato and commercially available orange and grapefruit
218 juice were purchased from local supermarkets. The fruits and vegetables were
219 chopped into small pieces and processed. Accurately weighted portions of fruits
220 and vegetable samples and aliquots of juice samples were spiked with the assayed
221 pesticides. The semi-solid samples (processed tangerine, lemon and tomato) were
222 blended with water. The pH of the pesticides-spiked samples was adjusted to
223 neutral by addition of a solution of NaOH. Each sample was centrifuged for 10 min
224 at 4000 g, the supernatant was diluted with methanol and the sample was
225 centrifuged again in the same conditions. Finally, each sample was filtered twice
226 prior to injection: first through a 0.45 μm nylon filter and then through a 0.22 μm
227 nylon filter.

228

229 **3.7. HPLC procedure**

The data matrices were collected using wavelengths from 200 to 350 nm each 1 nm, and each 1.6 s in the elution time axis. The slit width was 1 nm. The time-absorption matrices were of size 356 × 151 and were saved in ASCII format, and transferred to a PC for subsequent manipulation.

The mobile phase used for all chromatographic runs was a 50:50 (v/v) mixture of water and methanol, delivered at a flow rate of 1.0 mL min^{-1} with a chromatographic system operating under isocratic mode. Each chromatogram was accomplished in 9.5 minutes.

4. Results and discussion

4.1. Analysis of the calibration set

Using pure analyte standards, a chromatographic method allowing their partial separation was developed, making proper selection of the range of detected wavelengths and the composition of the mobile phase, in order to obtain an overall chromatographic time of less than 10 min. Under these conditions, when calibration samples were eluted, a cluster of coeluting peaks and two individual, fully resolved peaks appeared in all chromatographic runs (Fig. 2). Specifically, the MCR-ALS algorithm was used to process LC–DAD matrices taken at specific elution time ranges. Each chromatographic data matrix was divided in the following time regions: region I (3.3–6.9 min) and region II (7.3–9.5 min). These regions were delimited taking into account the spectrum of each analyte (Fig. 3), i.e., the wavelength ranges required to resolve them. Region I includes the four first eluted analytes: MBC, TBZ, PRO and FBZ. The spectrum of these analytes show that the high sensitivity range is from 250 nm to 350 nm, thus the wavelength range from

200 nm to 249 nm was discarded in their analysis. However, region II includes the last eluted analyte, CBL, whose maximum absorption peak is at 220 nm. In this region, the full wavelength range was selected.

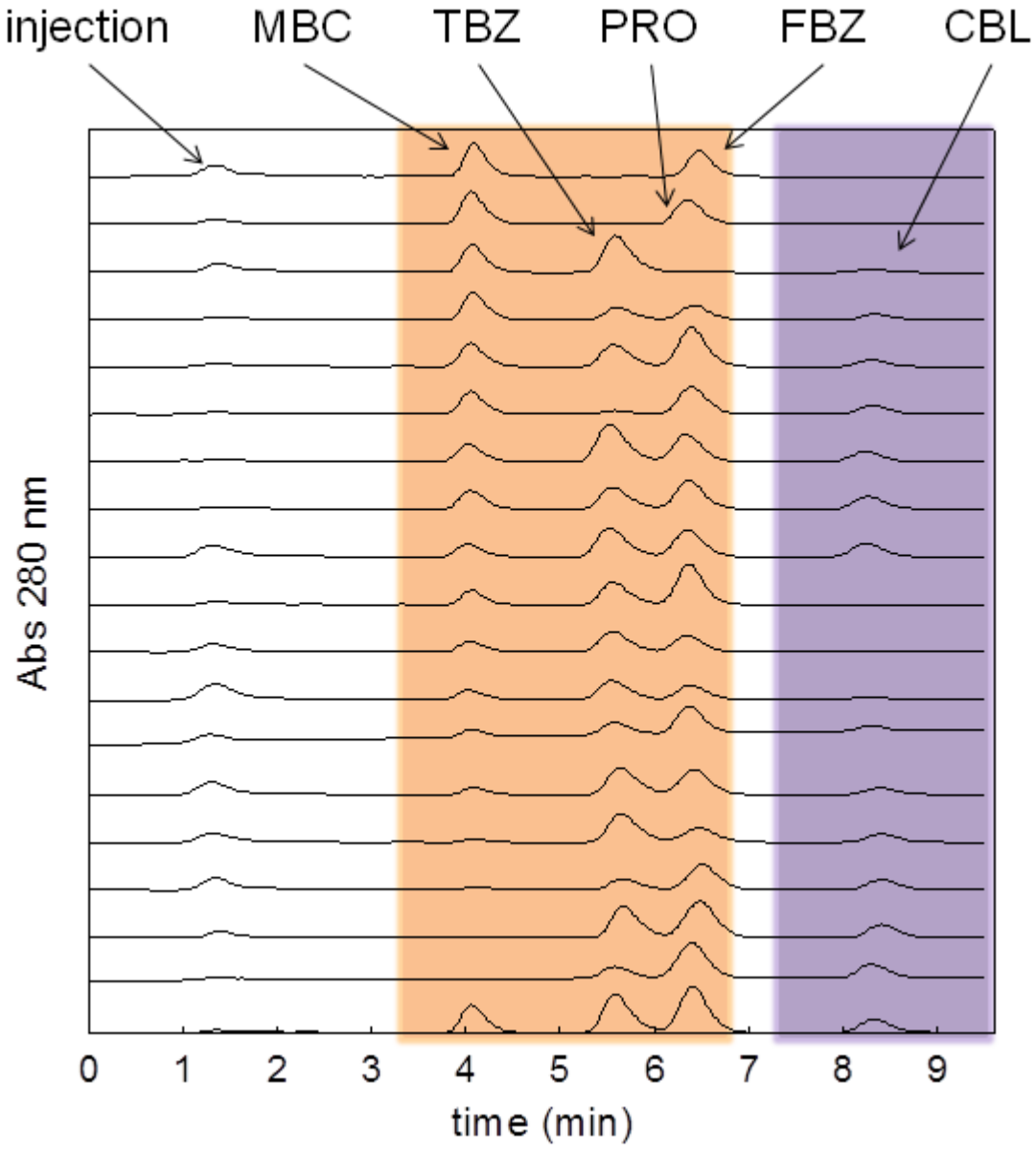

Figure 2

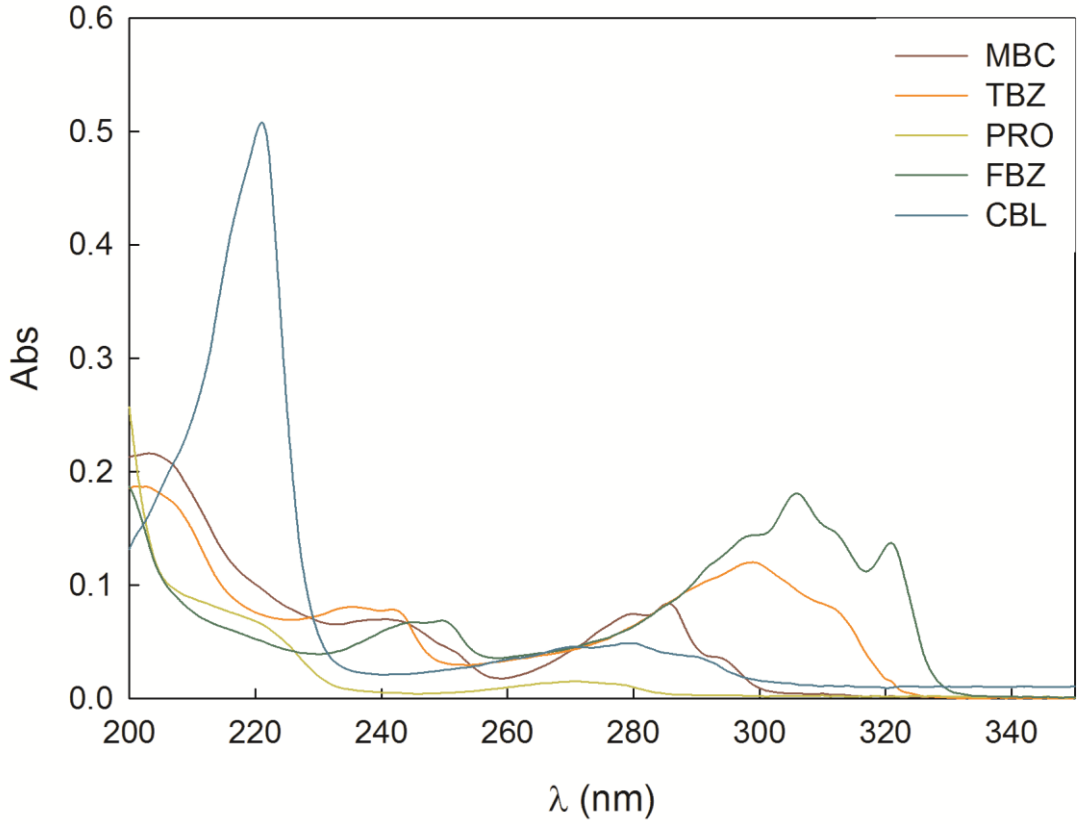

Figure 3

Notice in Fig. 2 that the the analyte elution time profiles significantly shift from run to run. This effect, combined with the presence of potential interferents in some of the analyzed samples, makes it difficult to align the chromatograms in the time mode, in order to restore the trilinearity required by some second-order multivariate algorithms. This is the main reason for employing the MCR–ALS algorithm for data processing. For each time region, MCR–ALS was applied to augmented matrices in the elution time direction, corresponding to the simultaneous analysis of the HPLC–DAD data matrices for the calibration set of samples. In this analysis, initialization of the multivariate algorithm was performed

using spectral estimates obtained from the analysis of the purest variables. Non-negativity restriction was applied in both modes; unimodality restriction was applied in the elution time mode only to the signals corresponding to the analytes (not to the background signal) but correspondence restriction was not applied during the ALS optimization phase.

The number of components was estimated by means of principal component analysis (PCA). The estimated number of components was five in region I and two in region II, which can be justified taking into account the presence of five different signals (corresponding to MBC, TBZ, PRO, FBZ and a background signal) in region I and two different signals (corresponding to CBL and a background signal) in region II. The resolution of calibration samples provided the characteristic chromatographic profiles and pure spectra for the different analytes plus one signal corresponding to a background. The number of iterations was less than 10 in all cases, with a residual fit lower than 0.07 mUA (region I) and 0.1 mUA (region II). Both residual fits are on the order of the expected instrumental noise associated with DAD detection.

After MCR–ALS resolution of the augmented calibration matrix, a pseudo-univariate calibration was carried out for each compound. The parameters corresponding to the linear regression of the scores from Eq. (5) vs. the corresponding nominal concentrations are shown in Table 2.

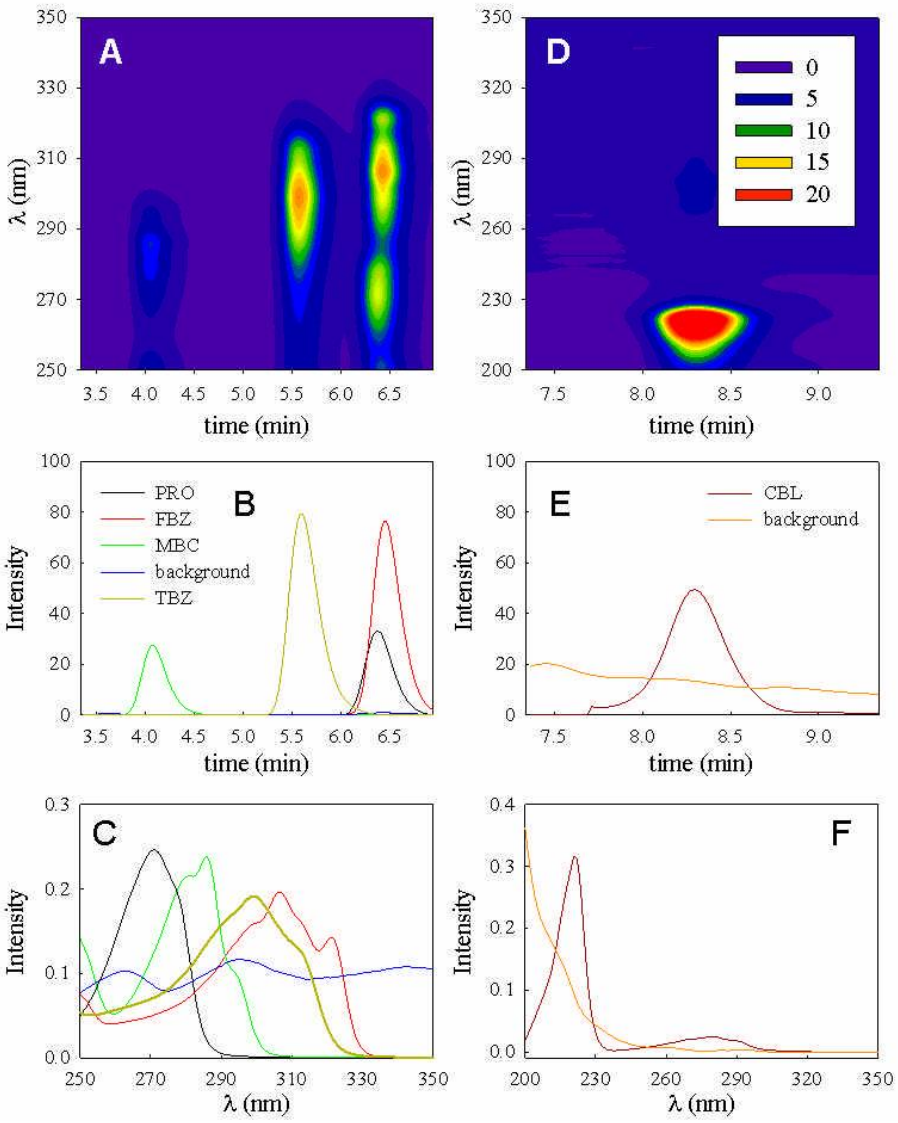

Figure 4

Region I corresponds to the fully overlapped peaks for PRO and FBZ, the partially overlapped peak for TBZ and also to the isolated peak for MBC (Fig. 4A). Five different independent contributions were resolved by MCR–ALS in the first peak cluster, corresponding to region I (Fig. 4A). For a typical sample, the five MCR–ALS resolved elution profiles are shown in Fig. 4B, and the spectra (common

300 to all samples) in Fig. 4C. These five contributions were identified as the analytes
301 MBC, TBZ, PRO, FBZ and a background signal by comparison of the MCR-
302 obtained spectra with the actual spectra of the pure compounds (Fig. 3).
303 Coelutions shown in Fig. 4A are untreatable by traditional chromatography;
304 however, mathematical resolution using MCR–ALS was still possible by processing
305 second-order HPLC–DAD data.

306 Region II contained a fully resolved peak at 8.3 min belonging to CBL. The
307 analysis of CBL was done both by the traditional method of area measurements
308 and by applying MCR–ALS to the sub-matrix containing its isolated peak. There
309 were not significant differences between the results obtained in both ways
310 ($p=0.337$). Figure 4D, 4E and 4F show the contour plot, the chromatogram and
311 spectrum corresponding to this region.

312

313 **4.2. Analysis of the validation set**

314 As indicated above, data matrices were analyzed by creating augmented
315 matrices with sub-matrices corresponding to specific time and wavelength windows
316 (regions I and II). For quantifying the analytes in the validation set of samples, each
317 validation HPLC–DAD data matrix was divided into the two selected regions. For
318 each time region, a time mode augmented matrix was created. Each augmented
319 matrix contained, adjacent to each other, the sub-matrices corresponding to the
320 validation samples and to the calibration samples. As before, non-negativity in both
321 modes and unimodality in the time mode (but not correspondence) were applied
322 during ALS optimization. Unimodality was only applied to the signal corresponding
323 to the analytes but not to the background signals. After optimization with the

multivariate algorithm, the scores corresponding to each analyte in each validation sample were isolated, and prediction proceeded by interpolation into the pseudo-univariate score-concentration calibration plot. Linear relationships between MCR–ALS scores and nominal concentrations were found in all cases, supported by the linearity test recommended by IUPAC [39]. The statistical results when MCR–ALS was applied to this validation set are shown in Table 2, implying linearity for all analytes.

As can be observed in Table 3, the predictions for the five analytes are in good agreement with the corresponding nominal values. The root mean square error of prediction (RMSEP) and the relative errors of prediction (REP), computed with respect to the mean calibration concentration of each analyte, can be calculated as follows:

$$\mathrm{RMSEP} = \sqrt{\frac{\sum_{t=1}^{T}(y_{\mathrm{pred},t} - y_{\mathrm{nom},t})^2}{T}} \quad (6)$$

$$\mathrm{REP} = 100\frac{\mathrm{RMSEP}}{\bar{y}_{\mathrm{cal}}} \quad (7)$$

where $y_{\mathrm{pred},t}$ is the predicted concentration in each sample, $y_{\mathrm{nom},t}$ is the nominal value of the concentration in the sample, T is he number of test samples, and $\bar{y}_{\mathrm{cal}}$ is the mean calibration concentration. The RMSEP and REP values are also quoted in Table 3. The limits of detection (LOD) and limits of quantification (LOQ) were calculated taking into account the errors of the slope and intercept of the pseudo-univariate calibration curves, as was previously reported by Saurina *et al* [40].

346

347 **4.3. Analysis of spiked real samples**

348 Official regulating agencies recommend maximum residue levels (MRL) for
349 the presently studied pesticides which are listed in Table 4 for the assayed fruits
350 and vegetables samples. As can be seen, these values are higher than the
351 calculated LOD (Table 3), and thus analyte pre-concentration is not required.

352 Real fruit and vegetable samples were spiked with these five pesticides and
353 were subjected to the analytical protocol discussed above. The estimated number
354 of components was seven or eight in region I and four in region II, i.e., there are
355 additional components in comparison to the calibration and validation samples.
356 Therefore, the analysis of these samples revealed that there are various interfering
357 species in each region, depending on the sample.

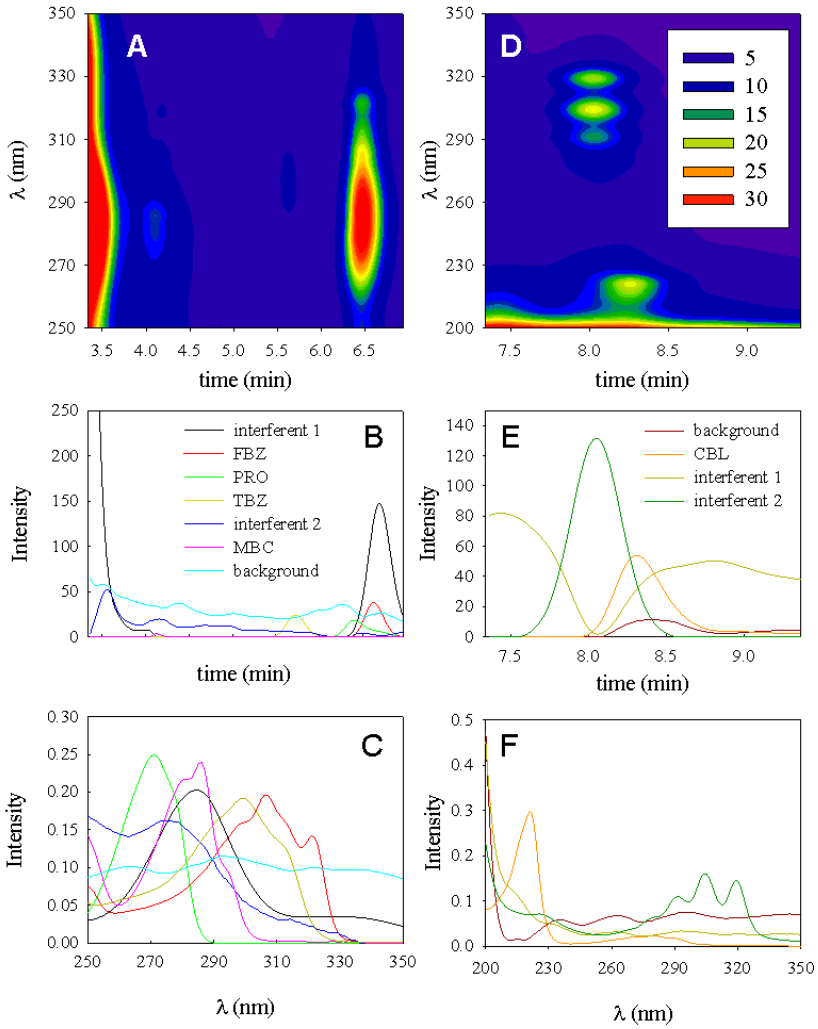

Figure 5

Each data matrix was divided into the two selected regions. As before, non-negativity in both modes and unimodality in the time mode were applied during ALS optimization. Unimodality was only applied to the signal corresponding to the analytes but not to the background signals or to the signals corresponding to interferents. In fact, some of the signals corresponding to interferents have more than one maximum in the time mode. This may be indicating that the interferents are not unique compounds, but also a combination of compounds with similar UV

spectra that cannot be resolved by MCR. As regards the correspondence restriction (which informs MCR-ALS that the potential interferents are absent in the calibration samples), it is interesting that there was no significant difference when applying correspondence or when this restriction was not applied. The number of iterations was less than 100 in all cases, with a residual fit lower than 0.3 mUA (region I) and 0.45 mUA (region II).

Figure 5 (A to F) shows the contour plot, the chromatogram and spectrum corresponding to both regions for one sample of orange juice. As can be seen, the spectra corresponding to the interfering species were different to those corresponding to the pesticides, allowing their resolution. The recovery results corresponding to different levels of each pesticide the five type of sample assayed are collected in Table 4. As can be appreciated, the predictions for the analytes are in good agreement with the nominal values. If the elliptical joint confidence region is analyzed for the slope and intercept of plot of predicted vs. nominal concentrations we conclude that the ellipse includes the theoretically expected values of (1,0), indicating the accuracy of the used methodology (data not shown). Indeed, a paired t-test indicates no significant difference between the nominal concentrations and the predicted using the presently proposed methodology. The p values are also listed in Table 4. This strongly suggests that HPLC-DAD combined to MCR-ALS is a useful methodology for the analysis of these pesticides in commercial juices, fruit and vegetable samples.

5. Conclusions

Complex samples including strongly coeluting analytes, elution time shifts, band shape changes and presence of uncalibrated interferents have been analyzed by HPLC–DAD. The flexibility of the applied multivariate model (MCR–ALS) allows the prediction of the concentrations of five analytes in a set of validation samples. More importantly, in the most challenging analytical scenario, i.e., real vegetable and fruit samples, these five analytes were quantified within a coeluting cluster in the presence of unwanted and non calibrated signals, achieving the second-order advantage which is inherent to second-order HPLC–DAD information.

Acknowledgements

Financial support provided by the University of Rosario, CONICET and ANPCyT (Project No. PIP 2010-0084) is appreciated. Valeria Boeris is grateful to CONICET for her scholarship.

References

[1] S. Topuz, G. Özhan, B. Alpertunga, Food Control. 16 (2005), pp. 87-92.

[2] European Commission (http://ec.europa.eu/) Last accessed on 31st October, 2013.

[3] U.S. Department of Heath & Human Services. U.S. Food and Drug Administration (http://www.fda.gov/) Last accessed on 31st October, 2013.

[4] G.F. Pang, C.L. Fan, Y.M. Liu, Y.Z. Cao, J.J. Zhang, B.L. Fu, X.M. Li, Z.Y. Li, Y.P. Wu, Multi, Food Addit. Contam. 23 (2006), pp. 777-810.

[5] A. Bordagaray, R. Garcia-Arrona, E. Millan, Anal. Methods. 5 (2013), pp. 2565-2571.

[6] X.Y. Song, Y.P. Shi, J. Chen, Food Chem. 139 (2013), pp. 246-252.

[7] G. Rübensam, F. Barreto, R.B. Hoff, T.M. Pizzolato, Food Control. 29 (2013), pp. 55-60.

[8] C. Carrillo-Carrión, B.M. Simonet, M. Valcárcel, Anal. Chim. Acta. 692 (2011), pp. 103-108.

[9] A. Moral, M.D. Sicilia, S. Rubio, Anal. Chim. Acta. 650 (2009), pp. 207-213.

[10] G.E. Mercer, J.A. Hurlbut, J. AOAC Int. 87 (2004), pp. 1224-1236.

[11] R.J. Bushway, D.L. Brandon, A.H. Bates, L. Li, K.A. Larkin, B.S. Young, J. Agric. Food. Chem. 43 (1995), pp. 1407-1412.

[12] G.S. Nunes, M.P. Marco, M. Farré, D. Barceló, Anal. Chim. Acta. 387 (1999), pp. 245-253.

[13] J. Sun, T. Dong, Y. Zhang, S. Wang, Anal. Chim. Acta. 666 (2010), pp. 76-82.

[14] G.S. Nunes, D. Barceló, B.S. Grabaric, J.M. Díaz-Cruz, M.L. Ribeiro, Anal. Chim. Acta. 399 (1999), pp. 37-49.

[15] J. Caetano, S.A.S. Machado, Sens. Actuators, B. 129 (2008), pp. 40-46.

[16] Q. Wu, Q. Chang, C. Wu, H. Rao, X. Zeng, C. Wang, Z. Wang, J. Chromatogr. A. 1217 (2010), pp. 1773-1778.

[17] S. Broecker, F. Pragst, A. Bakdash, S. Herre, M. Tsokos, Forensic Sci. Int., 212 (2011), pp. 215-226.

[18] M.J. Rodríguez-Cuesta, R. Boqué, F.X. Rius, D. Picón Zamora, M. Martínez Galera, A. Garrido Frenich, Anal. Chim. Acta. 491 (2003), pp. 47-56.

[19] M.J. Rodríguez-Cuesta, R. Boqué, F.X. Rius, J.L. Martínez Vidal, A. Garrido Frenich, Chemom. Intell. Lab. Syst. 77 (2005), pp. 251-260.

[20] X.D. Qing, H.L. Wu, C.C. Nie, X.F. Yan, Y.N. Li, J.Y. Wang, R.Q. Yu, Talanta. 103 (2013), pp. 86–94.

[21] R.M. Maggio, P.C. Damiani, A.C. Olivieri, Talanta, 83 (2011), pp. 1173-1180.

[22] S.A. Bortolato, J.A. Arancibia, G.M. Escandar, Anal. Chem. 80 (2008), pp. 8276-8286.

[23] K.S. Booksh, B.R. Kowalski, Anal. Chem. 66 (1994), pp. 782A-791A.

[24] H. Obana, M. Okihashi, K. Akutsu, Y. Kitagawa, S. Hori, J. Agric. Food Chem. 50 (2002), pp. 4464-4467.

[25] S. Seccia, S. Albrizio, P. Fidente, D. Montesano, J. Chromatogr. A. 1218 (2011), pp. 1253-1259.

[26] M. Saraji, N. Tansazan, J. Sep. Sci. 32 (2009), pp. 4186-4192.

[27] Y. Zhou, G. Xu, F.F.K. Choi, L.S. Ding, Q.B. Han, J.Z. Song, C.F. Qiao, Q.S. Zhao, H.X. Xu, J. Chromatogr. A. 1216 (2009), pp. 4847-4858.

[28] A. Belmonte Vega, A. Garrido Frenich, J.L. Martínez Vidal, Anal. Chim. Acta. 538 (2005), pp. 117-127.

[29] M. Fernández, Y. Picó, J. Mañes, J. Chromatogr. A. 871 (2000), pp. 43-56.

[30] J. Jaumot, R. Gargallo, A. de Juan, R. Tauler, Chemom. Intell. Lab. Syst. 76 (2005), pp. 101-110.

[31] M. Maeder, A. Zilian, Chemom. Intell. Lab. Syst. 3 (1988), pp. 205-213.

[32] M. Maeder, Anal. Chem. 59 (1987), pp. 527-530.

[33] W. Windig, J. Guilment, Anal. Chem. 63 (1991), pp. 1425-1432.

[34] G.H. Golub, C.F. Van Loan, Matrix Computations, Johns Hopkins University Press, 1996.

[35] R. Tauler, A. Smilde, B. Kowalski, J. Chemom. 9 (1995), pp. 31-58.

[36] R. Tauler, M. Maeder, A. de Juan, Multiset Data Analysis: Extended Multivariate Curve Resolution, in: S.D. Brown, R. Tauler, B. Walczak (Eds.) Comprehensive Chemometrics, Elsevier, Oxford, 2009, pp. 473-505.

[37] MATLAB version 2011b, The Mathworks Inc., Natick, Massachussets, USA.

[38] A.C. Olivieri, H.L. Wu, R.Q. Yu, Chemom. Intell. Lab. Syst. 96 (2009), pp. 246-251.

[39] K. Danzer, L.A. Currie, Pure & Appl. Chem. 70 (1998), pp. 993-1014.

[40] J. Saurina, C. Leal, R. Compañó, M. Granados, M.D. Prat, R. Tauler, Anal. Chim. Acta. 432 (2001), pp. 241-251.

475 Table 1: Calibration concentrations ($\mu g\ L^{-1}$) for the five assayed analytes.

Sample	MBC	TBZ	PRO	FBZ	CBL
1	0.0	62.1	1376	79.4	136.0
2	0.0	165.6	1376	79.4	122.4
3	22.8	62.1	516	79.4	102.0
4	22.8	165.6	516	29.8	81.6
5	57.0	165.6	1376	29.8	68.0
6	57.0	62.1	1376	29.8	54.4
7	91.2	113.8	172	54.6	34.0
8	91.2	113.8	946	9.9	13.6
9	114.0	113.8	1720	54.6	0.0
10	114.0	165.6	516	79.4	136.0
11	136.8	113.8	946	54.6	122.4
12	136.8	207.0	946	54.6	102.0
13	171.0	20.7	946	54.6	81.6
14	171.0	113.8	946	99.2	68.0
15	205.2	62.1	516	29.8	54.4
16	205.2	207.0	0	0.0	34.0
17	228.0	0.0	1720	0.0	13.6
18	228.0	0.0	0	99.2	0.0

476

477

478 Table 2: Summary of the results from the pseudo-univariate calibration curves for

479 all analytes [a].

	Slope [b]	Intercept [b]	r^2	$s_{y/x}$	*p* value
MBC	1.48(3)	-2(4)	0.9833	14	0.161
TBZ	5.16(7)	11(9)	0.9894	29	0.464
PRO	0.252(4)	7(4)	0.9917	13	0.603
FBZ	9.8(2)	20(10)	0.9894	33	0.262
CBL	12.0(2)	-10(10)	0.9902	56	0.253

480

481 [a] r^2, squared correlation coefficient; $s_{y/x}$, standard deviation of regression residuals, *p* value,

482 probability associated to the IUPAC recommended *F* test for linearity ($p > 0.05$ implies linearity at

483 95% confidence level).

484 [b] Standard deviation in parenthesis.

485

Table 3: MCR–ALS results for the prediction of the studied analytes in the validation set of samples.

Sample	MBC (μg L^{-1})		TBZ (μg L^{-1})		PRO (μg L^{-1})		FBZ (μg L^{-1})		CBL (μg L^{-1})	
	N	P[a]	N	P[a]	N	P[a]	N	P[a]	N	P[a]
1	173.0	170(6)	95.2	87.1(2)	963	920(30)	9.9	10(2)	12.2	11.3(7)
2	166.0	165(4)	137.0	136(3)	1030	1070(10)	82.3	81(4)	121.0	123(3)
3	0.0	1.1(2)	149.0	146.7(4)	602	570(10)	32.7	31(3)	70.7	69(2)
4	228.0	234(7)	53.8	51(2)	1340	1240(60)	21.8	21(2)	96.6	94(2)
5	160.0	157(5)	164.0	158(3)	1170	1160(10)	71.4	71(4)	132.0	125(2)
6	77.5	75.8(4)	51.8	54.2(2)	1100	1100(10)	36.7	36.1(4)	44.9	46.1(9)
7	22.8	24(2)	176.0	185(2)	1340	1360(10)	45.6	44.6(4)	46.2	47.7(6)
8	166.0	166(5)	74.5	73(2)	654	603(8)	0.9	-	89.8	88(2)
9	185.0	188(5)	20.7	15.7(1)	1200	1180(20)	13.9	13(2)	20.4	20.5(9)
10	66.1	66(2)	186.0	185.8(3)	361	340(10)	54.6	55(3)	6.8	6(2)
RMSEP	2.6		4.7		43		0.85		2.6	
REP (%)	2.1		4.3		4.4		2.3		4.0	
LOD	2.3		0.90		12		0.46		0.32	
LOQ	6.9		2.7		36		1.4		1.1	
Sensitivity	0.092		0.24		0.018		0.47		1.2	
Selectivity	0.53		0.29		0.69		0.31		0.73	
Analytical sensitivity	1.4		3.7		0.28		7.2		2.9	

[a] Standard deviation in parenthesis. N = nominal, P = predicted.

Table 4: MCR–ALS results for the prediction of the studied analytes in the spiked samples.

Sample		MBC (μg L^{-1})		TBZ (μg L^{-1})		PRO (μg L^{-1})		FBZ (μg L^{-1})		CBL (μg L^{-1})	
		N	P[a]	N	P[a]	N	P[a]	N	P[a]	N	P[a]
Orange Juice	1	185.0	195(4)	16.6	15.9(7)	1170	1310(20)	79.4	72.2(7)	5.7	6.91(7)
	2	73.0	80(3)	10.4	12.2(7)	48	57(1)	30.8	28.1(4)	88.4	97(1)
	3	11.4	15(3)	47.6	43.1(8)	860	940(10)	34.7	35.3(4)	42.2	48.6(6)
	4	153.0	145(5)	93.1	84(2)	22	36(2)	12.9	8.1(3)	15.0	16.2(8)
	MRL	200		5000		50		50		10	
	RMSEP	7.6		5.2		81		4.5		5.4	
	REP (%)	6.6		4.9		9.2		8.9		8.0	
Grapefruit Juice	5	210.0	218(6)	76.6	72(4)	1030	1080(20)	41.7	44(1)	135.0	132(6)
	6	198.0	191(5)	201.0	205(8)	69	53(4)	14.9	11.8(6)	6.8	7.9(3)
	7	155.0	163(5)	153.0	160(6)	1720	1810(40)	77.4	81(2)	16.3	12.2(6)
	8	25.1	20.1(9)	64.2	70(3)	34	37(3)	45.6	42(2)	105.0	101(4)
	MRL	200		5000		50		50		10	
	RMSEP	7.2		5.5		52		3.2		3.1	
	REP (%)	6.4		5.1		5.8		6.3		4.6	
Lemon	9	160.0	151(3)	80.7	75(2)	224	250(10)	14.9	15.5(4)	40.8	38.8(9)
	10	66.1	70(2)	97.3	103(3)	172	180(10)	68.4	71(1)	72.1	75(2)
	11	228.0	239(5)	132.0	136(3)	1690	1670(20)	71.4	69(1)	69.4	64(2)
	12	29.6	30.1(6)	82.8	79(2)	654	690(20)	48.6	50.5(8)	6.8	7.5(7)
	MRL	700		5000		300		50		10	
	RMSEP	7.2		4.8		44		2.0		3.2	
	REP (%)	6.4		4.5		5.0		4.0		4.8	

This table continues in the next page.

494 Table 4 (continued)

Tangerine	13	132.0	125(3)	159.0	150(10)	1100	1070(20)	5.9	5.2(1)	132.0	125(2)
	14	198.0	204(5)	97.3	102(5)	1200	1140(20)	20.8	19(1)	15.0	12.1(2)
	15	93.5	97(2)	207.0	200(20)	430	440(10)	87.3	83(1)	80.2	78(1)
	16	59.3	64(2)	132.0	126(6)	155	125(7)	41.7	47(2)	6.8	6.6(3)
	MRL	700		5000		300		50		10	
	RMSEP	5.4		7.1		39		3.6		3.9	
	REP (%)	4.8		6.7		4.4		7.0		5.8	
Tomato	17	38.8	42(1)	84.9	87.6(9)	206	166(4)	21.8	29.6(4)	124.0	131(3)
	18	80.9	76(2)	97.3	91(1)	1010	970(10)	25.8	23.5(3)	8.2	9.8(2)
	19	108.0	115(2)	128.0	121(1)	740	797(8)	60.5	56.9(7)	59.8	65(2)
	20	213.0	203(3)	15.5	21.3(7)	17	38(7)	40.0	43.6(6)	24.5	21(2)
	MRL	300		50		50		50		10	
	RMSEP	6.8		5.8		43		4.8		4.8	
	REP (%)	5.9		5.4		4.9		9.5		7.1	
p value		0.389		0.206		0.794		0.439		0.694	

495

496 [a] Standard deviation in parenthesis. N = nominal, P = predicted.

497

Figure captions

Figure 1: Chemical structures of the five assayed pesticides.

Figure 2: Liquid chromatograms (λ of detection: 280 nm) for the set of calibration samples. The signal corresponding to each analyte was identified. The subregions selected are highlighted.

Figure 3: Spectra of pure standards of the five assayed pesticides in medium methanol-water (50:50 v/v). Pesticide concentration: 1 mg/L.

Figure 4: Results for the analysis of a calibration sample. (A) Surface plot around the first cluster peak (region I) containing the analytes MBC, TBZ, PRO and FBZ (B) MCR–ALS resolved elution profiles for the same sample, with all analytes indicated. (C) Spectral profiles retrieved by MCR–ALS analysis, which are common to all samples. (D) Surface plot around the region II containing CBL (E) MCR–ALS resolved elution profiles in region II. (F) Spectral profiles retrieved by MCR–ALS analysis.

Figure 5: Results for the analysis of an orange juice sample. (A) Surface plot around the first cluster peak (region I) containing the analytes MBC, TBZ, PRO and FBZ (B) MCR–ALS resolved elution profiles for the same sample, with all analytes indicated. (C) Spectral profiles retrieved by MCR–ALS analysis. (D) Surface plot

around the region II containing CBL (E) MCR–ALS resolved elution profiles in region II. (F) Spectral profiles retrieved by MCR–ALS analysis.

Determination of five pesticides in juice, fruit and vegetable samples by means of liquid chromatography combined with multivariate curve resolution

Valeria Boeris, Juan A. Arancibia, Alejandro C. Olivieri

Departamento de Química Analítica, Facultad de Ciencias Bioquímicas y Farmacéuticas, Universidad Nacional de Rosario e Instituto de Química Rosario (IQUIR-CONICET), Suipacha 531(S2002LRK) Rosario, Argentina.

Corresponding author:

Alejandro Olivieri

Tel./fax: +54 3414372704.

E-mail addresses: olivieri@iquir-conicet.gov.ar, aolivier@fbioyf.unr.edu.ar

Abstract

The aim of this work was to quantify five commonly used pesticides (propoxur, carbaryl, carbendazim, thiabendazole and fuberidazole) in real samples as: tomato, orange juice, grapefruit juice, lemon and tangerine. The method used for the determination of these analytes in the complex matrices was high-performance liquid chromatography with diode array detection. In order to work under isocratic conditions and to complete each run in less than 10 min, the analysis was carried out applying multivariate curve resolution coupled to alternating least-squares (MCR–ALS). The flexibility of this applied multivariate model allowed the prediction of the concentrations of the five analytes in complex samples including strongly coeluting analytes, elution time shifts, band shape changes and presence of uncalibrated interferents. The obtained limits of detection (in $\mu g\ L^{-1}$) using the proposed methodology were 2.3 (carbendazim), 0.90 (thiabendazole), 12 (propoxur), 0.46 (fuberidazole) and 0.32 (carbaryl).

Keywords

High-performance liquid chromatography; Diode array detection; Multivariate curve resolution; Pesticides; Vegetable samples

Abbreviations

High-performance liquid chromatography (HPLC), diode array detection (DAD), multivariate curve resolution coupled to alternating least-squares (MCR-ALS),

propoxur (PRO), carbaryl (CBL), carbendazim (MBC), thiabendazole (TBZ), fuberidazole (FBZ)

1. Introduction

Although the use of pesticides provides unquestionable benefits in providing a plentiful, low-cost supply of high-quality fruits and vegetables, their incorrect application may leave harmful residues, which involve possible health risk [1]. The concentration of pesticides is regulated in many samples such as drinking waters, vegetables, juices, etc., by the European Commission [2] and the Food and Drug Administration [3], among other agencies. Traditionally, the instrumental techniques employed to determine these compounds involve fluorescence, gas or liquid chromatography [4-8]. Specifically, the determination of benzimidazolic pesticides (carbendazim, thiabendazole and fuberidazole) and/or carbamates (carbaryl, propoxur and carbendazim) in fruits and vegetables have been carried out by various approaches, such as supramolecular solvent-based microextraction followed by high-performance liquid chromatography (HPLC) with fluorescence detection [9], gas chromatography coupled to mass spectrometry and selected ion monitoring [10], enzymatic immunoassay using antibodies [11-13] or electrochemical methods [14, 15].

The analysis of mixtures of pesticides using methods based on ~~high-performance liquid chromatography (~~HPLC~~)~~ sometimes results in complex separations and overlapped peaks [16, 17]. Nevertheless, complex multicomponent mixtures can in many cases be qualitatively and quantitatively resolved by means of chemometrics. Depending on their nature, data can be

arranged in a two-way structure (a table or a matrix), as in the case of collecting the absorbance spectra for many samples, or in a three-way structure, e.g. in HPLC with diode array detection (DAD), where spectra are recorded at several elution times for each sample. Such data arrangements in three- or higher way arrays can be handled using multi-way methods of analysis [18, 19].

Collection of multi-dimensional chromatographic information, and data processing by advanced chemometric algorithms constitute a fruitful combination of techniques, recently applied to diverse research areas [20-22]. Chemometrics is required whenever perfect separation of the various sample components cannot be achieved by the employed chromatographic system, leading to overlapping peaks in the elution time mode. In these cases, selectivity may be mathematically restored by applying multivariate data analysis [23]. In particular, the so-called second-order advantage can be achieved, a property which is inherent to matrix instrumental data, and implies that analytes can be quantified in samples containing potential interferences [21]. Signals arising from coeluting analytes or foreign components can be modeled by powerful second-order multivariate algorithms.

The combination of chemometrics to HPLC presents additional advantages in relation to traditional methods: since chemometrics allows resolving coeluted peaks, it is possible to reduce the duration of the chromatographic run, allowing not only processing more samples but also reducing the solvent consumption, saving time and money. Moreover, several authors report that gradient of solvents was required to achieve resolution of the analytes [24-26]: this requirement may be

avoided using isocratic conditions and resolving the peak by applying chemometrics.

In liquid chromatographic runs, elution time shifts and band shape changes usually occur from sample to sample: in these cases, a useful alternative is to analyze the data with flexible algorithms, which allow a given component to present different time profiles in different samples, such as parallel factor analysis 2 (PARAFAC2) or multivariate curve resolution coupled to alternating least-squares (MCR-ALS) [27]. Recent work from our laboratory indicated better performance with MCR–ALS in the case of multi-analyte quantification in the presence of high overlapping of elution profiles and uncalibrated interferences, mainly because of the possibility of building a more constrained model in MCR–ALS in comparison with PARAFAC2 [22].

In the present report, we selected MCR–ALS as the algorithm of choice for processing HPLC-DAD data, and discuss its behavior towards the quantification of the following five pesticides in fruit and vegetable samples: propoxur (PRO), carbaryl (CBL), carbendazim (MBC), thiabendazole (TBZ) and fuberidazole (FBZ) (Fig. 1). The presence of benzimidazoles, carbamates and their degradation products in waters or food products is potentially harmful for humans due to their proven toxicity. This is the cause of the continued interest in the development of analytical methods for monitoring these families of compounds. Previous chromatographic analysis of the presently studied compounds required up to 35 min [28, 29]. The aim of this work is to quantify these analytes in complex matrices under HPLC isocratic conditions and in less than 10 min.

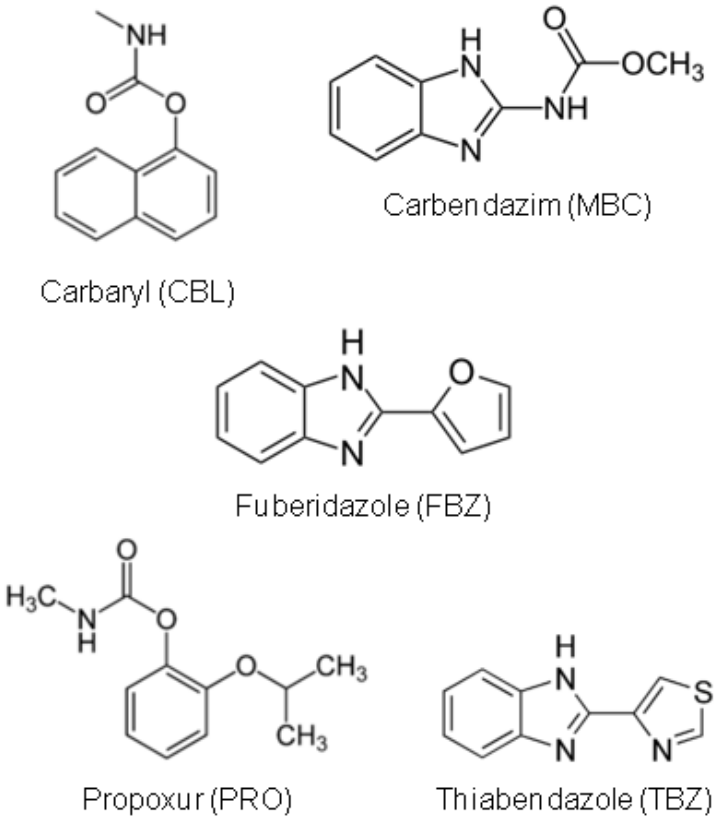

Figure 1

2. Theory

The bilinear model assumed by MCR methods is analogous to the generalized Lambert-Beer's law, where the individual responses of each component are additive. In matrix form, this bilinear model is expressed as:

$$\mathbf{D} = \mathbf{C}\,\mathbf{S}^{T} + \mathbf{E} \quad (1)$$

where **D** (size $J \times K$) is the matrix of experimental data (J is the number of elution time data points and K is the number of absorption wavelengths), **C** (size $J \times N$) is the matrix whose columns contain the concentration profiles of the N components present in the samples, $\mathbf{S}^{T}$ (size $N \times K$) is the matrix whose rows contain the

component spectra and **E** (size $J \times K$) is a matrix collecting the experimental error and the variance not explained by the bilinear model of equation (1).

The first step in MCR-ALS studies is to obtain a rough estimation of the number of components, which can be simply performed by visual inspection of singular values or principal component analysis (PCA) [30, 31]. ~~plots for the matrix of experimental data. This initial number of components can be then refined if necessary, i.e., increasing or decreasing the number of components, depending on their fit and chemical reasonability.~~

The resolution is accomplished using an iterative ALS procedure, initialized using an initial estimation of the spectral or concentration profiles for each intervening species. Different methods are used for this purpose, such as evolving factor analysis [32] or the determination of the purest variables [33]. If the initial estimations are the spectral profiles, the unconstrained least-squares solution for the concentration profiles can be calculated from the expression:

$$\mathbf{C} = \mathbf{D}\,(\mathbf{S}^{T})^{+} \qquad (2)$$

where $(\mathbf{S}^{T})^{+}$ is the pseudoinverse of the spectral matrix $\mathbf{S}^{T}$, ~~which is equal to $[\mathbf{S}(\mathbf{S}^{T}\mathbf{S})^{-1}]$ when $\mathbf{S}^{T}$ is full rank~~ [34]. If the initial estimations were the concentration profiles, the unconstrained least-squares solution for the spectra can be calculated from the expression:

$$\mathbf{S}^{T} = \mathbf{C}^{+}\,\mathbf{D} \qquad (3)$$

where $\mathbf{C}^{+}$ is the pseudoinverse of **C** ~~$[\mathbf{C}^{+} = (\mathbf{C}^{T}\mathbf{C})^{-1}\mathbf{C}^{T}]$, when **C** is full rank~~. Both steps can be implemented in an alternating least-squares cycle, so that, at each iteration, new **C** and $\mathbf{S}^{T}$ matrices are obtained. During these iterative

recalculations of **C** and $\mathbf{S}^T$, a series of constraints ~~are~~ (e.g. non-negativity, unimodality and sample selectivity; the latter removes a component which is known to be absent in a given sample) could be applied to give physical meaning to the obtained solutions, and to limit their possible number for the same data fitting and decrease the extent of possible rotation ambiguities [35]. Iterations continue until an optimal solution is obtained that fulfils the postulated constraints and the established convergence criteria. ~~Non-negativity constraints may be applied to the concentration profiles, due to the fact that the concentrations of the chemical species are always positive values or zero. Non-negativity constraints can also applied for UV-Vis spectra. Unimodality is a constraint which can be applied to profiles having a single maximum, as in the case of chromatographic profiles.~~

The procedure described above can be easily extended to the simultaneous analysis of multiple data sets or data matrices if they have at least one data mode (direction) in common. For instance, if the different data sets have been analyzed by the same spectroscopic method, the possible data arrangement and bilinear model extension is given by the following equation:

$$\mathbf{D}_{aug} = \begin{bmatrix} \mathbf{D}_{cal1} \\ \mathbf{D}_{cal2} \\ \cdots \\ \mathbf{D}_{test} \end{bmatrix} = \begin{bmatrix} \mathbf{C}_{cal1} \\ \mathbf{C}_{cal2} \\ \cdots \\ \mathbf{C}_{test} \end{bmatrix} \mathbf{S}^T + \begin{bmatrix} \mathbf{E}_{cal1} \\ \mathbf{E}_{cal2} \\ \cdots \\ \mathbf{E}_{test} \end{bmatrix} = \mathbf{C}_{aug}\mathbf{S}^T + \mathbf{E}_{aug} \quad (4)$$

where $\mathbf{D}_{aug}$ is the augmented data matrix, constructed from *I* individual data matrices [36], corresponding to the set of calibration samples ($\mathbf{D}_{cal1}$, $\mathbf{D}_{cal2}$, ...) and to a single test sample ($\mathbf{D}_{test}$). ~~Each of these data matrices has size *J*×*K*, where *J* is the number of rows and *K* is the number of columns. In this column-wise~~

augmentation mode, the data matrices are placed on top of each other, giving the matrix $\mathbf{D}_{aug}$ of size $IJ \times K$, which keeps the same number of columns in all of them, and where the different data matrices share their column vector space, $\mathbf{C}_{aug}$ is the column-wise augmented matrix of size $IJ \times N$, and $\mathbf{E}_{aug}$ is the corresponding augmented error matrix. This extended MCR-ALS approach can be used to obtain quantitative determination of an analyte in the presence of other sample components (e.g. interferents).

In this case, $\mathbf{C}_{aug}$ is the column-wise augmented matrix of concentration profiles (size $JI \times N$, where N is the number of responsive chemical components), $\mathbf{S}^T$ is the matrix of loadings (dimensions $N \times K$) in the row vector space, and $\mathbf{E}_{aug}$ collects the residuals. After decomposition, the scores for analyte n are computed as the sum of the elements of the corresponding profile in each of the sub-matrices of $\mathbf{C}_{aug}$. Specifically, the analyte calibration score in the calibration sample i ($a_{cali,n}$) is calculated from the elements of the $\mathbf{C}_{cali}$ matrix, which corresponds to the analyte in each calibration sample:

$$a_{\mathrm{cal}i,n} = \sum_{j=1}^{J} c_{\mathrm{cal}i}(j,n) \quad (5)$$

where cal$i$ identifies the calibration sample, n the component of interest, j each of the data points or channels in the sub-matrix along the non-augmented mode and $c_{cali}(j,n)$ the element of the $\mathbf{C}_{cali}$ matrix at channel j for component n. On the other hand, the analyte score in the test sample ($a_{test,n}$) is defined analogously from the $\mathbf{C}_{test}$ matrix, which corresponds to the analyte in the test sample:

$$a_{\mathrm{test},n} = \sum_{j=1}^{J} c_{\mathrm{test}}(j,n) \quad (6)$$

where $c_{test}(j,n)$ is an element of the $\mathbf{C}_{test}$ matrix [see equation (4)].

Finally, the calibration scores are employed to build a pseudo-univariate calibration line, leading to an estimation of the corresponding slope (m_n) and offset (n_n). The analyte score in the test sample is then interpolated in the calibration line to yield the predicted analyte concentration c_n:

$$c_n = (a_{test,n} - n_n) / m_n \quad (5)$$

In extended MCR-ALS analysis, another useful constraint which can be applied is the so-called correspondence or sample selectivity, which informs the algorithm that certain components are absent in some samples, e.g., potential interferents may be present in the unknowns but absent in the calibration samples.

3. Experimental

3.1. Reagents

Carbendazim (MBC), thiabendazole (TBZ), fuberidazole (FBZ), propoxur (PRO) and carbaryl (CBL) were purchased from Sigma Aldrich Co. (St. Louis, MO). Methanol was obtained from Merck. Milli-Q water (Millipore) was used in all experiments. Solvents were filtered through 0.45 µm filters.

3.2. Stock standard and working standard solutions

Stock standard solutions of MBC (570 mg L^{-1}), TBZ (1150 mg L^{-1}), FBZ (620 mg L^{-1}), PRO (1720 mg L^{-1}) and CBL (680 mg L^{-1}) were prepared in 25.00 mL volumetric flasks by dissolving accurately weighed amounts of the drugs in methanol and completing to the mark with the same solvent. From these solutions, more diluted solutions were obtained (MBC 22.8 mg L^{-1}, TBZ 20.7 mg L^{-1}, FBZ

9.92 mg L^{-1}, PRO 172 mg L^{-1}, CBL 13.6 mg L^{-1}). Working solutions were prepared immediately before their use by taking appropriate aliquots of solutions and diluting with methanol and water (50:50 v/v) to the desired concentrations.

3.3. Apparatus

Chromatographic runs were performed on an HP 1200 liquid chromatograph (Agilent Technologies, Waldbronn, Germany) consisting of a quaternary pump, a manual injector fitted with a 200 µL loop and a diode array UV–visible detector set at a wavelength range from 200 to 350 nm. A C18 column of 150mm×4.6mm, 5µm particle size was employed (Agilent Sorbax SB). The data were collected using the software HP ChemStation for LC Rev.HP 1990–1997.

3.4. Software

The data were handled using the MATLAB computer environment [37]. The calculations involved in the mixture resolution by MCR-ALS have been made using mvc2_gui, a MATLAB graphical interface toolbox which is a new version of that already reported in the literature [38].

3.5. Calibration and validation samples

In order to design the calibration set, preliminary experiments were performed with the pure analytes, showing that the full elution time range could be divided into three relevant regions: an overlapped zone where three analytes appear (TBZ, PRO and FBZ) and two regions where the remaining two analytes are fully resolved (MBC and CRL). A set of 18 calibration solutions containing the

231 analytes in the ranges 0 - 228 μg L^{-1} for MBC, 0 - 207 μg L^{-1} for TBZ, 0 - 1720 μg L^{-1} for PRO, 0 – 99.2 μg L^{-1} for FBZ and 0 - 136 μg L^{-1} for CBL were prepared in appropriate volumetric flasks. The concentrations are collected in Table 1. Fifteen of these samples correspond to the concentrations provided by a central composite design for the three analytes appearing in the overlapped region: TBZ, PRO and FBZ. Each of the remaining three samples of the 18-sample set corresponds to each of the three pure analytes at their maximum levels. Each of these 18 samples was combined with nine equally spaced, duplicate concentration levels for the two resolved analytes. For establishing the calibration concentration ranges, the linear range for all components was studied by analyzing different solutions covering the interval 0–2000 μg L^{-1}.

A validation set of 10 samples was also prepared, containing the five analytes in concentrations different than those used for calibration, and following a random design, i.e., the specific concentrations were taken as random numbers generated within the calibration domain.

3.6. Samples and sample preparation

Tangerine, lemon, tomato and commercially available orange and grapefruit juice were purchased from local supermarkets. The fruits and vegetables were chopped into small pieces and processed. Accurately weighted portions of fruits and vegetable samples and aliquots of juice samples were spiked with the assayed pesticides. The semi-solid samples (processed tangerine, lemon and tomato) were blended with water. The pH of the pesticides-spiked samples was adjusted to

neutral by addition of a solution of NaOH. Each sample was centrifuged for 10 min at 4000 g, the supernatant was diluted with methanol and the sample was centrifuged again in the same conditions. Finally, each sample was filtered twice prior to injection: first through a 0.45 μm nylon filter and then through a 0.22 μm nylon filter.

3.7. HPLC procedure

The data matrices were collected using wavelengths from 200 to 350 nm each 1 nm, and each 1.6 s in the elution time axis. The slit width was 1 nm. The time-absorption matrices were of size 356 × 151 and were saved in ASCII format, and transferred to a PC for subsequent manipulation.

The mobile phase used for all chromatographic runs was a 50:50 (v/v) mixture of water and methanol, delivered at a flow rate of 1.0 mL min^{-1} with a chromatographic system operating under isocratic mode. Each chromatogram was accomplished in 9.5 minutes.

4. Results and discussion

4.1. Analysis of the calibration set

Using pure analyte standards, a chromatographic method allowing their partial separation was developed, making proper selection of the range of detected wavelengths and the composition of the mobile phase, in order to obtain an overall chromatographic time of less than 10 min. Under these conditions, when calibration samples were eluted, a cluster of coeluting peaks and two individual,

277 fully resolved peaks appeared in all chromatographic runs (Fig. 2). Specifically, the
278 MCR-ALS algorithm was used to process LC–DAD matrices taken at specific
279 elution time ranges. Each chromatographic data matrix was divided in the following
280 time regions: region I (3.3–6.9 min) and region II (7.3–9.5 min). These regions
281 were delimited taking into account the spectrum of each analyte (Fig. 3), i.e., the
282 wavelength ranges required to resolve them. Region I includes the four first eluted
283 analytes: MBC, TBZ, PRO and FBZ. The spectrum of these analytes show that the
284 high sensitivity range is from 250 nm to 350 nm, thus the wavelength range from
285 200 nm to 249 nm was discarded in their analysis. However, region II includes the
286 last eluted analyte, CBL, whose maximum absorption peak is at 220 nm. In this
287 region, the full wavelength range was selected.
288

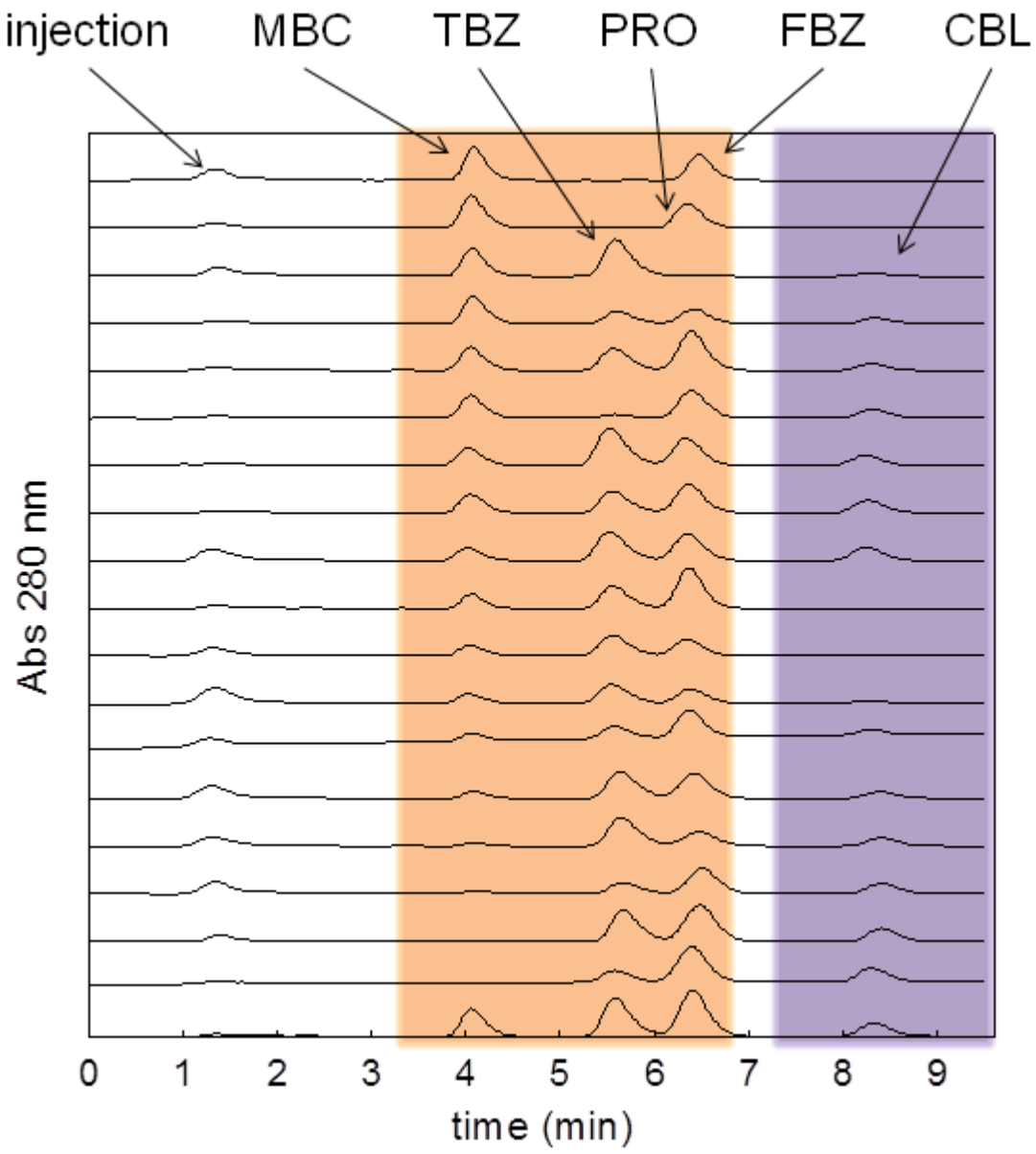

289

290 Figure 2

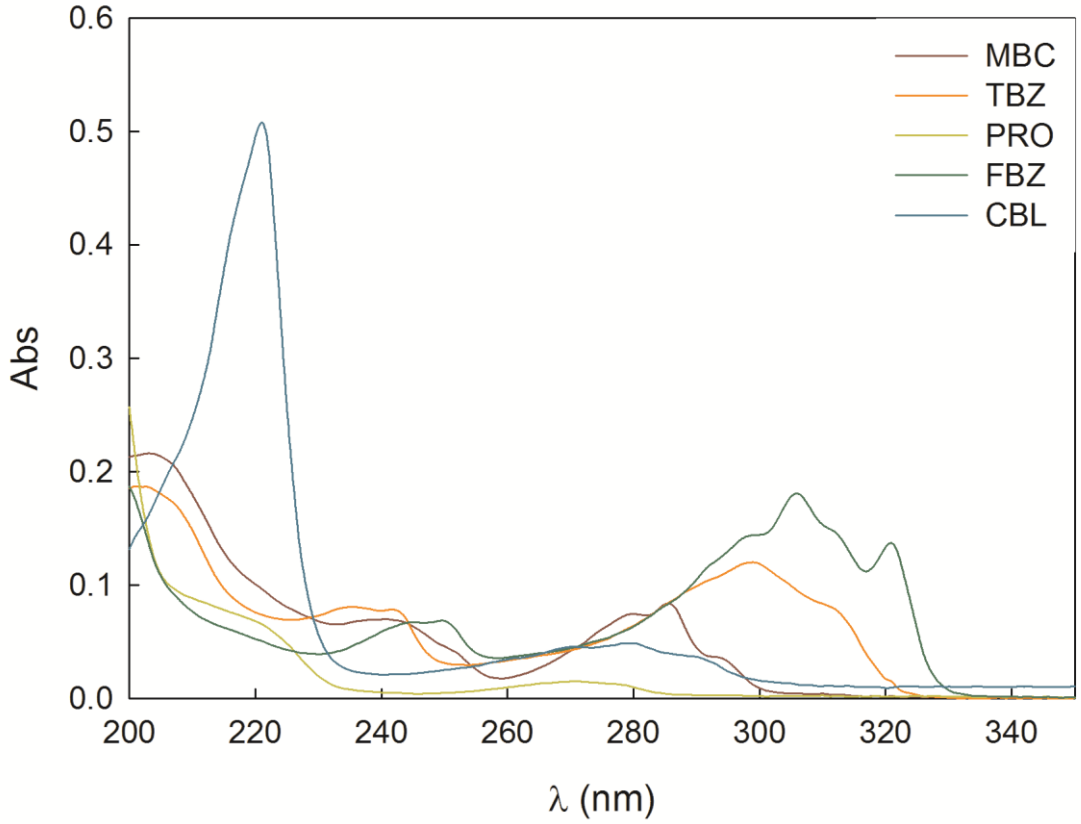

Figure 3

Notice in Fig. 2 that the the analyte elution time profiles significantly shift from run to run. This effect, combined with the presence of potential interferents in some of the analyzed samples, makes it difficult to align the chromatograms in the time mode, in order to restore the trilinearity required by some second-order multivariate algorithms. This is the main reason for employing the MCR–ALS algorithm for data processing. For each time region, MCR–ALS was applied to augmented matrices in the elution time direction, corresponding to the simultaneous analysis of the HPLC–DAD data matrices for the calibration set of samples. In this analysis, initialization of the multivariate algorithm was performed

using spectral estimates obtained from the analysis of the purest variables. Non-negativity restriction was applied in both modes; unimodality restriction was applied in the elution time mode only to the signals corresponding to the analytes (not to the background signal) but correspondence restriction was not applied during the ALS optimization phase.

The number of components was estimated by means of principal component analysis (PCA). ~~PCA is a mathematical procedure that uses orthogonal transformation to convert a set of observations of possibly correlated variables into a set of values of linearly uncorrelated variables called principal components: the first principal component has the largest possible variance (that is, accounts for as much of the variability in the data as possible), and each succeeding component in turn has the highest variance possible under the constraint that it be orthogonal to the preceding components.~~ The estimated number of components was five in region I and two in region II, which can be justified taking into account the presence of five different signals (corresponding to MBC, TBZ, PRO, FBZ and a background signal) in region I and two different signals (corresponding to CBL and a background signal) in region II. The resolution of calibration samples provided the characteristic chromatographic profiles and pure spectra for the different analytes plus one signal corresponding to a background. The number of iterations was less than 10 in all cases, with a residual fit lower than 0.07 mUA (region I) and 0.1 mUA (region II). Both residual fits are on the order of the expected instrumental noise associated with DAD detection.

After MCR–ALS resolution of the augmented calibration matrix, a pseudo-univariate calibration was carried out for each compound. The parameters

corresponding to the linear regression of the scores from Eq. (5) vs. the corresponding nominal concentrations are shown in Table 2.

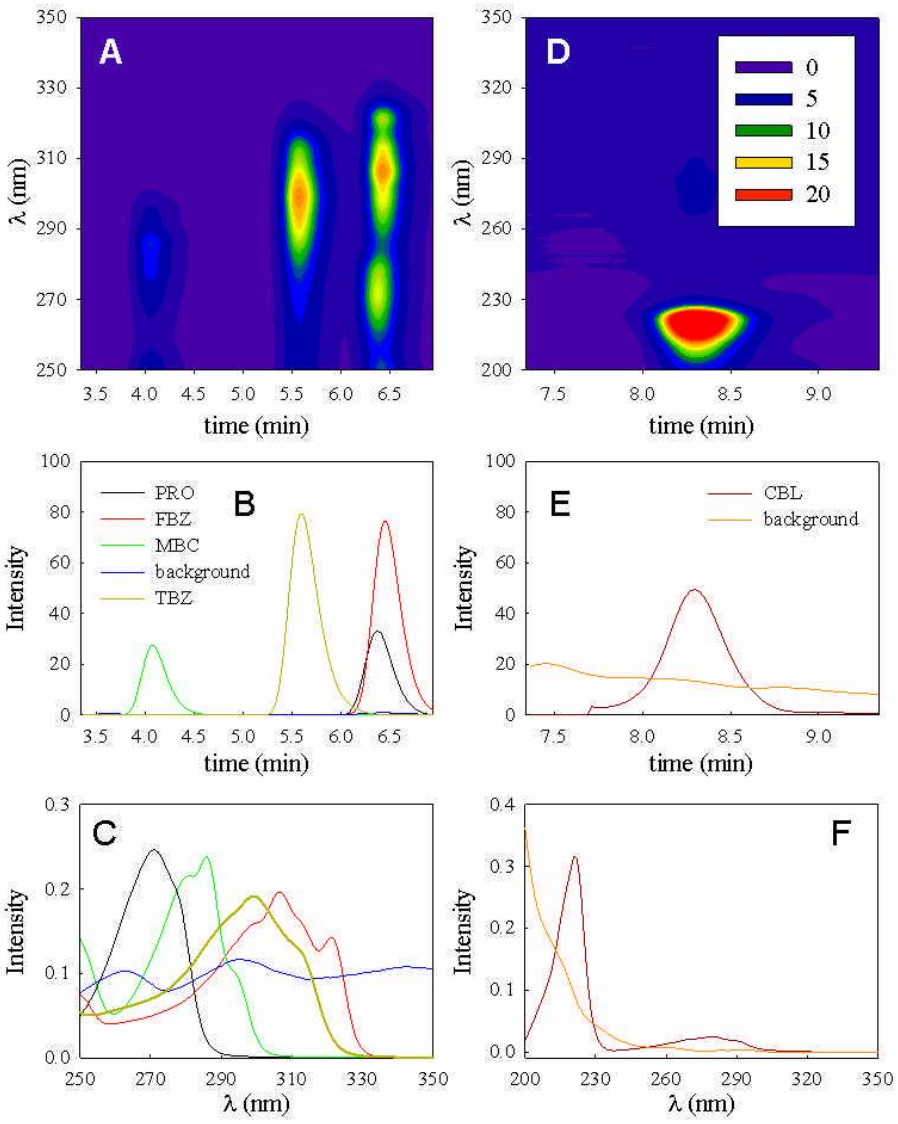

Figure 4

Region I corresponds to the fully overlapped peaks for PRO and FBZ, the partially overlapped peak for TBZ and also to the isolated peak for MBC (Fig. 4A). Five different independent contributions were resolved by MCR–ALS in the first

peak cluster, corresponding to region I (Fig. 4A). For a typical sample, the five MCR–ALS resolved elution profiles are shown in Fig. 4B, and the spectra (common to all samples) in Fig. 4C. These five contributions were identified as the analytes MBC, TBZ, PRO, FBZ and a background signal by comparison of the MCR-obtained spectra with the actual spectra of the pure compounds (Fig. 3). Coelutions shown in Fig. 4A are untreatable by traditional chromatography; however, mathematical resolution using MCR–ALS was still possible by processing second-order HPLC–DAD data.

Region II contained a fully resolved peak at 8.3 min belonging to CBL. The analysis of CBL was done both by the traditional method of area measurements and by applying MCR–ALS to the sub-matrix containing its isolated peak. There were not significant differences between the results obtained in both ways ($p=0.337$). Figure 4D, 4E and 4F show the contour plot, the chromatogram and spectrum corresponding to this region.

4.2. Analysis of the validation set

As indicated above, data matrices were analyzed by creating augmented matrices with sub-matrices corresponding to specific time and wavelength windows (regions I and II). For quantifying the analytes in the validation set of samples, each validation HPLC–DAD data matrix was divided into the two selected regions. For each time region, a time mode augmented matrix was created. Each augmented matrix contained, adjacent to each other, the sub-matrices corresponding to the validation samples and to the calibration samples. As before, non-negativity in both modes and unimodality in the time mode (but not correspondence) were applied

during ALS optimization. Unimodality was only applied to the signal corresponding to the analytes but not to the background signals. After optimization with the multivariate algorithm, the scores corresponding to each analyte in each validation sample were isolated, and prediction proceeded by interpolation into the pseudo-univariate score-concentration calibration plot. ~~Good~~ Linear relationships between MCR–ALS scores and nominal concentrations were found in all cases, supported by the linearity test recommended by IUPAC [39]. The statistical results when MCR–ALS was applied to this validation set are shown in Table 2, implying linearity for all analytes.

As can be observed in Table 3, the predictions for the five analytes are in good agreement with the corresponding nominal values. The root mean square error of prediction (RMSEP) and the relative errors of prediction (REP), computed with respect to the mean calibration concentration of each analyte, can be calculated as follows:

$$\mathrm{RMSEP} = \sqrt{\frac{\sum_{t=1}^{T}(y_{pred,t} - y_{nom,t})^2}{T}} \quad (6)$$

$$\mathrm{REP} = 100\frac{\mathrm{RMSEP}}{\bar{y}_{cal}} \quad (7)$$

where $y_{pred,t}$ is the predicted concentration in each sample, $y_{nom,t}$ is the nominal value of the concentration in the sample, T is he number of test samples, and $\bar{y}_{cal}$ is the mean calibration concentration. The RMSEP and REP values are also quoted in Table 3. The limits of detection (LOD) and limits of quantification (LOQ) were calculated taking into account the errors of the slope and intercept of the

pseudo-univariate calibration curves, as was previously reported by Saurina *et al* [40].

4.3. Analysis of spiked real samples

Official regulating agencies recommend maximum residue levels (MRL) for the presently studied pesticides which are listed in Table 4 for the assayed fruits and vegetables samples. As can be seen, these values are higher than the calculated LOD (Table 3), and thus analyte pre-concentration is not required.

Real fruit and vegetable samples were spiked with these five pesticides and were subjected to the analytical protocol discussed above. The estimated number of components was seven or eight in region I and four in region II, i.e., there are additional components in comparison to the calibration and validation samples. Therefore, the analysis of these samples revealed that there are various interfering species in each region, depending on the sample.

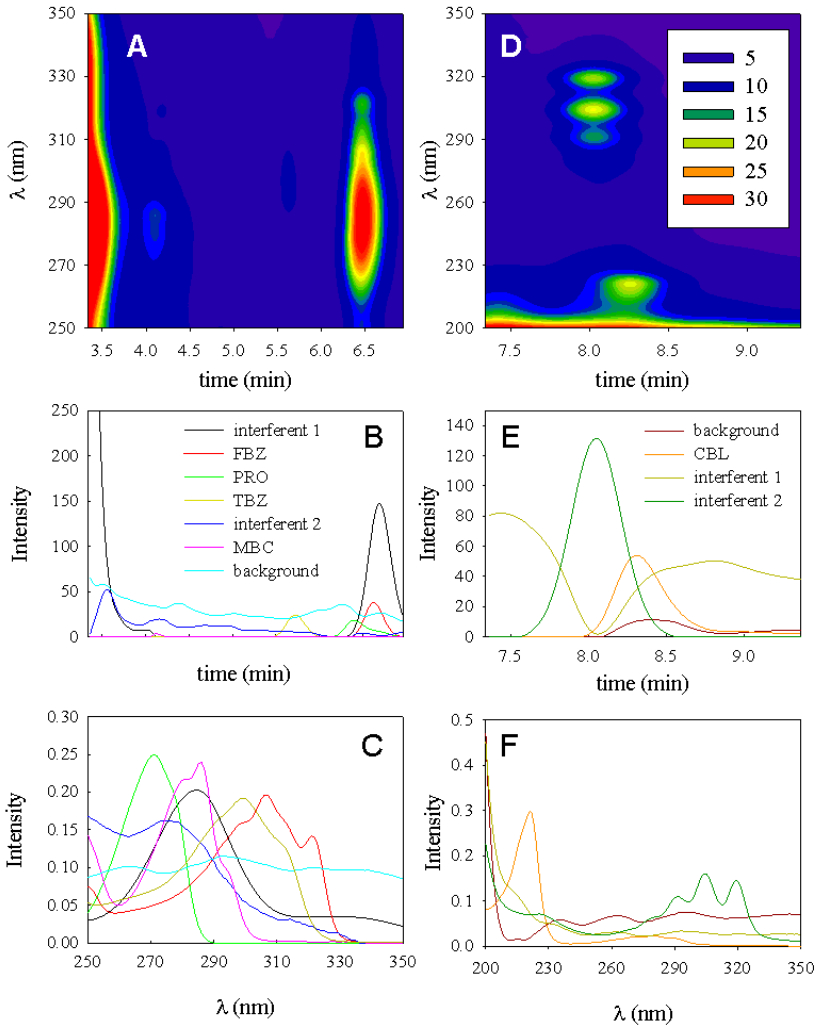

Figure 5

Each data matrix was divided into the two selected regions. As before, non-negativity in both modes and unimodality in the time mode were applied during ALS optimization. Unimodality was only applied to the signal corresponding to the analytes but not to the background signals or to the signals corresponding to interferents. In fact, some of the signals corresponding to interferents have more than one maximum in the time mode. This may be indicating that the interferents are not unique compounds, but also a combination of compounds with similar UV

spectra that cannot be resolved by MCR. As regards the correspondence restriction (which informs MCR-ALS that the potential interferents are absent in the calibration samples), it is interesting that there was no significant difference when applying correspondence or when this restriction was not applied. The number of iterations was less than 100 in all cases, with a residual fit lower than 0.3 mUA (region I) and 0.45 mUA (region II).

Figure 5 (A to F) shows the contour plot, the chromatogram and spectrum corresponding to both regions for one sample of orange juice. As can be seen, the spectra corresponding to the interfering species were different to those corresponding to the pesticides, allowing their resolution. The recovery results corresponding to different levels of each pesticide the five type of sample assayed are collected in Table 4. As can be appreciated, the predictions for the analytes are in good agreement with the nominal values. If the elliptical joint confidence region is analyzed for the slope and intercept of plot of predicted vs. nominal concentrations we conclude that the ellipse includes the theoretically expected values of (1,0), indicating the accuracy of the used methodology (data not shown). Indeed, a paired t-test indicates no significant difference between the nominal concentrations and the predicted using the presently proposed methodology. The p values are also listed in Table 4. This strongly suggests that HPLC-DAD combined to MCR-ALS is a useful methodology for the analysis of these pesticides in commercial juices, fruit and vegetable samples.

5. Conclusions

Complex samples including strongly coeluting analytes, elution time shifts, band shape changes and presence of uncalibrated interferents have been analyzed by HPLC–DAD. The flexibility of the applied multivariate model (MCR–ALS) allows the prediction of the concentrations of five analytes in a set of validation samples. More importantly, in the most challenging analytical scenario, i.e., real vegetable and fruit samples, these five analytes were quantified within a coeluting cluster in the presence of unwanted and non calibrated signals, achieving the second-order advantage which is inherent to second-order HPLC–DAD information.

Acknowledgements

Financial support provided by the University of Rosario, CONICET and ANPCyT (Project No. PIP 2010-0084) is appreciated. Valeria Boeris is grateful to CONICET for her scholarship.

References

[1] S. Topuz, G. Özhan, B. Alpertunga, Food Control. 16 (2005), pp. 87-92.

[2] European Commission (http://ec.europa.eu/) Last accessed on 31st October, 2013.

[3] U.S. Department of Heath & Human Services. U.S. Food and Drug Administration (http://www.fda.gov/) Last accessed on 31st October, 2013.

[4] G.F. Pang, C.L. Fan, Y.M. Liu, Y.Z. Cao, J.J. Zhang, B.L. Fu, X.M. Li, Z.Y. Li, Y.P. Wu, Multi, Food Addit. Contam. 23 (2006), pp. 777-810.

[5] A. Bordagaray, R. Garcia-Arrona, E. Millan, Anal. Methods. 5 (2013), pp. 2565-2571.

[6] X.Y. Song, Y.P. Shi, J. Chen, Food Chem. 139 (2013), pp. 246-252.

[7] G. Rübensam, F. Barreto, R.B. Hoff, T.M. Pizzolato, Food Control. 29 (2013), pp. 55-60.

[8] C. Carrillo-Carrión, B.M. Simonet, M. Valcárcel, Anal. Chim. Acta. 692 (2011), pp. 103-108.

[9] A. Moral, M.D. Sicilia, S. Rubio, Anal. Chim. Acta. 650 (2009), pp. 207-213.

[10] G.E. Mercer, J.A. Hurlbut, J. AOAC Int. 87 (2004), pp. 1224-1236.

[11] R.J. Bushway, D.L. Brandon, A.H. Bates, L. Li, K.A. Larkin, B.S. Young, J. Agric. Food. Chem. 43 (1995), pp. 1407-1412.

[12] G.S. Nunes, M.P. Marco, M. Farré, D. Barceló, Anal. Chim. Acta. 387 (1999), pp. 245-253.

[13] J. Sun, T. Dong, Y. Zhang, S. Wang, Anal. Chim. Acta. 666 (2010), pp. 76-82.

[14] G.S. Nunes, D. Barceló, B.S. Grabaric, J.M. Díaz-Cruz, M.L. Ribeiro, Anal. Chim. Acta. 399 (1999), pp. 37-49.

468 [15] J. Caetano, S.A.S. Machado, Sens. Actuators, B. 129 (2008), pp. 40-46.
469 [16] Q. Wu, Q. Chang, C. Wu, H. Rao, X. Zeng, C. Wang, Z. Wang, J. Chromatogr.
470 A. 1217 (2010), pp. 1773-1778.
471 [17] S. Broecker, F. Pragst, A. Bakdash, S. Herre, M. Tsokos, Forensic Sci. Int.,
472 212 (2011), pp. 215-226.
473 [18] M.J. Rodríguez-Cuesta, R. Boqué, F.X. Rius, D. Picón Zamora, M. Martínez
474 Galera, A. Garrido Frenich, Anal. Chim. Acta. 491 (2003), pp. 47-56.
475 [19] M.J. Rodríguez-Cuesta, R. Boqué, F.X. Rius, J.L. Martínez Vidal, A. Garrido
476 Frenich, Chemom. Intell. Lab. Syst. 77 (2005), pp. 251-260.
477 [20] X.D. Qing, H.L. Wu, C.C. Nie, X.F. Yan, Y.N. Li, J.Y. Wang, R.Q. Yu, Talanta.
478 103 (2013), pp. 86–94.
479 [21] R.M. Maggio, P.C. Damiani, A.C. Olivieri, Talanta, 83 (2011), pp. 1173-1180.
480 [22] S.A. Bortolato, J.A. Arancibia, G.M. Escandar, Anal. Chem. 80 (2008), pp.
481 8276-8286.
482 [23] K.S. Booksh, B.R. Kowalski, Anal. Chem. 66 (1994), pp. 782A-791A.
483 [24] H. Obana, M. Okihashi, K. Akutsu, Y. Kitagawa, S. Hori, J. Agric. Food Chem.
484 50 (2002), pp. 4464-4467.
485 [25] S. Seccia, S. Albrizio, P. Fidente, D. Montesano, J. Chromatogr. A. 1218
486 (2011), pp. 1253-1259.
487 [26] M. Saraji, N. Tansazan, J. Sep. Sci. 32 (2009), pp. 4186-4192.
488 [27] Y. Zhou, G. Xu, F.F.K. Choi, L.S. Ding, Q.B. Han, J.Z. Song, C.F. Qiao, Q.S.
489 Zhao, H.X. Xu, J. Chromatogr. A. 1216 (2009), pp. 4847-4858.
490 [28] A. Belmonte Vega, A. Garrido Frenich, J.L. Martínez Vidal, Anal. Chim. Acta.
491 538 (2005), pp. 117-127.

[29] M. Fernández, Y. Picó, J. Mañes, J. Chromatogr. A. 871 (2000), pp. 43-56.

[30] J. Jaumot, R. Gargallo, A. de Juan, R. Tauler, Chemom. Intell. Lab. Syst. 76 (2005), pp. 101-110.

[31] M. Maeder, A. Zilian, Chemom. Intell. Lab. Syst. 3 (1988), pp. 205-213.

[32] M. Maeder, Anal. Chem. 59 (1987), pp. 527-530.

[33] W. Windig, J. Guilment, Anal. Chem. 63 (1991), pp. 1425-1432.

[34] G.H. Golub, C.F. Van Loan, Matrix Computations, Johns Hopkins University Press, 1996.

[35] R. Tauler, A. Smilde, B. Kowalski, J. Chemom. 9 (1995), pp. 31-58.

[36] R. Tauler, M. Maeder, A. de Juan, Multiset Data Analysis: Extended Multivariate Curve Resolution, in: S.D. Brown, R. Tauler, B. Walczak (Eds.) Comprehensive Chemometrics, Elsevier, Oxford, 2009, pp. 473-505.

[37] MATLAB version 2011b, The Mathworks Inc., Natick, Massachussets, USA.

[38] A.C. Olivieri, H.L. Wu, R.Q. Yu, Chemom. Intell. Lab. Syst. 96 (2009), pp. 246-251.

[39] K. Danzer, L.A. Currie, Pure & Appl. Chem. 70 (1998), pp. 993-1014.

[40] J. Saurina, C. Leal, R. Compañó, M. Granados, M.D. Prat, R. Tauler, Anal. Chim. Acta. 432 (2001), pp. 241-251.

511 Table 1: Calibration concentrations ($\mu g\ L^{-1}$) for the five assayed analytes.

Sample	MBC	TBZ	PRO	FBZ	CBL
1	0.0	62.1	1376	79.4	136.0
2	0.0	165.6	1376	79.4	122.4
3	22.8	62.1	516	79.4	102.0
4	22.8	165.6	516	29.8	81.6
5	57.0	165.6	1376	29.8	68.0
6	57.0	62.1	1376	29.8	54.4
7	91.2	113.8	172	54.6	34.0
8	91.2	113.8	946	9.9	13.6
9	114.0	113.8	1720	54.6	0.0
10	114.0	165.6	516	79.4	136.0
11	136.8	113.8	946	54.6	122.4
12	136.8	207.0	946	54.6	102.0
13	171.0	20.7	946	54.6	81.6
14	171.0	113.8	946	99.2	68.0
15	205.2	62.1	516	29.8	54.4
16	205.2	207.0	0	0.0	34.0
17	228.0	0.0	1720	0.0	13.6
18	228.0	0.0	0	99.2	0.0

512

513

514 Table 2: Summary of the results from the pseudo-univariate calibration curves for

515 all analytes [a].

	Slope [b]	Intercept [b]	r^2	$s_{y/x}$	*p* value
MBC	1.48(3)	-2(4)	0.9833	14	0.161
TBZ	5.16(7)	11(9)	0.9894	29	0.464
PRO	0.252(4)	7(4)	0.9917	13	0.603
FBZ	9.8(2)	20(10)	0.9894	33	0.262
CBL	12.0(2)	-10(10)	0.9902	56	0.253

516

517 [a] r^2, squared correlation coefficient; $s_{y/x}$, standard deviation of regression residuals, *p* value,

518 probability associated to the IUPAC recommended *F* test for linearity ($p > 0.05$ implies linearity at

519 95% confidence level).

520 [b] Standard deviation in parenthesis.

521

522 Table 3: MCR–ALS results for the prediction of the studied analytes in the validation set of samples.

Sample	MBC (μg L^{-1})		TBZ (μg L^{-1})		PRO (μg L^{-1})		FBZ (μg L^{-1})		CBL (μg L^{-1})	
	N	P[a]	N	P[a]	N	P[a]	N	P[a]	N	P[a]
1	173.0	170(6)	95.2	87.1(2)	963	920(30)	9.9	10(2)	12.2	11.3(7)
2	166.0	165(4)	137.0	136(3)	1030	1070(10)	82.3	81(4)	121.0	123(3)
3	0.0	1.1(2)	149.0	146.7(4)	602	570(10)	32.7	31(3)	70.7	69(2)
4	228.0	234(7)	53.8	51(2)	1340	1240(60)	21.8	21(2)	96.6	94(2)
5	160.0	157(5)	164.0	158(3)	1170	1160(10)	71.4	71(4)	132.0	125(2)
6	77.5	75.8(4)	51.8	54.2(2)	1100	1100(10)	36.7	36.1(4)	44.9	46.1(9)
7	22.8	24(2)	176.0	185(2)	1340	1360(10)	45.6	44.6(4)	46.2	47.7(6)
8	166.0	166(5)	74.5	73(2)	654	603(8)	0.9	-	89.8	88(2)
9	185.0	188(5)	20.7	15.7(1)	1200	1180(20)	13.9	13(2)	20.4	20.5(9)
10	66.1	66(2)	186.0	185.8(3)	361	340(10)	54.6	55(3)	6.8	6(2)
RMSEP	2.6		4.7		43		0.85		2.6	
REP (%)	2.1		4.3		4.4		2.3		4.0	
LOD	2.3		0.90		12		0.46		0.32	
LOQ	6.9		2.7		36		1.4		1.1	
Sensitivity	0.092		0.24		0.018		0.47		1.2	
Selectivity	0.53		0.29		0.69		0.31		0.73	
Analytical sensitivity	1.4		3.7		0.28		7.2		2.9	

523

524 [a] Standard deviation in parenthesis. N = nominal, P = predicted.

525

526 Table 4: MCR–ALS results for the prediction of the studied analytes in the spiked samples.

Sample		MBC (μg L^{-1})		TBZ (μg L^{-1})		PRO (μg L^{-1})		FBZ (μg L^{-1})		CBL (μg L^{-1})	
		N	P[a]	N	P[a]	N	P[a]	N	P[a]	N	P[a]
Orange Juice	1	185.0	195(4)	16.6	15.9(7)	1170	1310(20)	79.4	72.2(7)	5.7	6.91(7)
	2	73.0	80(3)	10.4	12.2(7)	48	57(1)	30.8	28.1(4)	88.4	97(1)
	3	11.4	15(3)	47.6	43.1(8)	860	940(10)	34.7	35.3(4)	42.2	48.6(6)
	4	153.0	145(5)	93.1	84(2)	22	36(2)	12.9	8.1(3)	15.0	16.2(8)
	MRL	200		5000		50		50		10	
	RMSEP	7.6		5.2		81		4.5		5.4	
	REP (%)	6.6		4.9		9.2		8.9		8.0	
Grapefruit Juice	5	210.0	218(6)	76.6	72(4)	1030	1080(20)	41.7	44(1)	135.0	132(6)
	6	198.0	191(5)	201.0	205(8)	69	53(4)	14.9	11.8(6)	6.8	7.9(3)
	7	155.0	163(5)	153.0	160(6)	1720	1810(40)	77.4	81(2)	16.3	12.2(6)
	8	25.1	20.1(9)	64.2	70(3)	34	37(3)	45.6	42(2)	105.0	101(4)
	MRL	200		5000		50		50		10	
	RMSEP	7.2		5.5		52		3.2		3.1	
	REP (%)	6.4		5.1		5.8		6.3		4.6	
Lemon	9	160.0	151(3)	80.7	75(2)	224	250(10)	14.9	15.5(4)	40.8	38.8(9)
	10	66.1	70(2)	97.3	103(3)	172	180(10)	68.4	71(1)	72.1	75(2)
	11	228.0	239(5)	132.0	136(3)	1690	1670(20)	71.4	69(1)	69.4	64(2)
	12	29.6	30.1(6)	82.8	79(2)	654	690(20)	48.6	50.5(8)	6.8	7.5(7)
	MRL	700		5000		300		50		10	
	RMSEP	7.2		4.8		44		2.0		3.2	
	REP (%)	6.4		4.5		5.0		4.0		4.8	

527

528 This table continues in the next page.

529

530 Table 4 (continued)

Tangerine	13	132.0	125(3)	159.0	150(10)	1100	1070(20)	5.9	5.2(1)	132.0	125(2)
	14	198.0	204(5)	97.3	102(5)	1200	1140(20)	20.8	19(1)	15.0	12.1(2)
	15	93.5	97(2)	207.0	200(20)	430	440(10)	87.3	83(1)	80.2	78(1)
	16	59.3	64(2)	132.0	126(6)	155	125(7)	41.7	47(2)	6.8	6.6(3)
	MRL	700		5000		300		50		10	
	RMSEP	5.4		7.1		39		3.6		3.9	
	REP (%)	4.8		6.7		4.4		7.0		5.8	
Tomato	17	38.8	42(1)	84.9	87.6(9)	206	166(4)	21.8	29.6(4)	124.0	131(3)
	18	80.9	76(2)	97.3	91(1)	1010	970(10)	25.8	23.5(3)	8.2	9.8(2)
	19	108.0	115(2)	128.0	121(1)	740	797(8)	60.5	56.9(7)	59.8	65(2)
	20	213.0	203(3)	15.5	21.3(7)	17	38(7)	40.0	43.6(6)	24.5	21(2)
	MRL	300		50		50		50		10	
	RMSEP	6.8		5.8		43		4.8		4.8	
	REP (%)	5.9		5.4		4.9		9.5		7.1	
p value		0.389		0.206		0.794		0.439		0.694	

531

532 [a] Standard deviation in parenthesis. N = nominal, P = predicted.

533

Figure captions

Figure 1: Chemical structures of the five assayed pesticides.

Figure 2: Liquid chromatograms (λ of detection: 280 nm) for the set of calibration samples. The signal corresponding to each analyte was identified. The subregions selected are highlighted.

Figure 3: Spectra of pure standards of the five assayed pesticides in medium methanol-water (50:50 v/v). Pesticide concentration: 1 mg/L.

Figure 4: Results for the analysis of a calibration sample. (A) Surface plot around the first cluster peak (region I) containing the analytes MBC, TBZ, PRO and FBZ (B) MCR–ALS resolved elution profiles for the same sample, with all analytes indicated. (C) Spectral profiles retrieved by MCR–ALS analysis, which are common to all samples. (D) Surface plot around the region II containing CBL (E) MCR–ALS resolved elution profiles in region II. (F) Spectral profiles retrieved by MCR–ALS analysis.

Figure 5: Results for the analysis of an orange juice sample. (A) Surface plot around the first cluster peak (region I) containing the analytes MBC, TBZ, PRO and FBZ (B) MCR–ALS resolved elution profiles for the same sample, with all analytes indicated. (C) Spectral profiles retrieved by MCR–ALS analysis. (D) Surface plot

around the region II containing CBL (E) MCR–ALS resolved elution profiles in region II. (F) Spectral profiles retrieved by MCR–ALS analysis.

Figure 1

Click here to download high resolution image

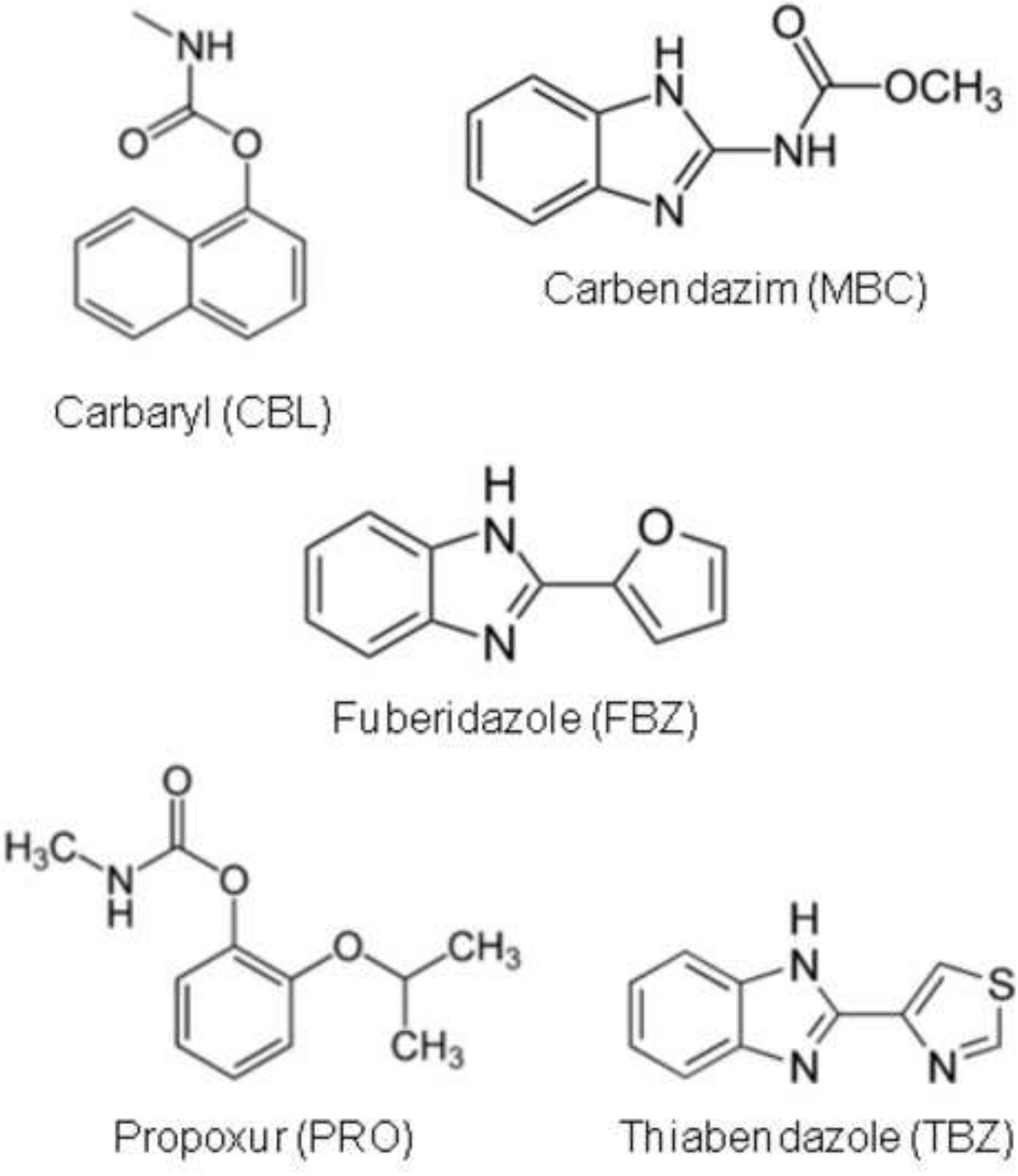

Figure 2

Click here to download high resolution image

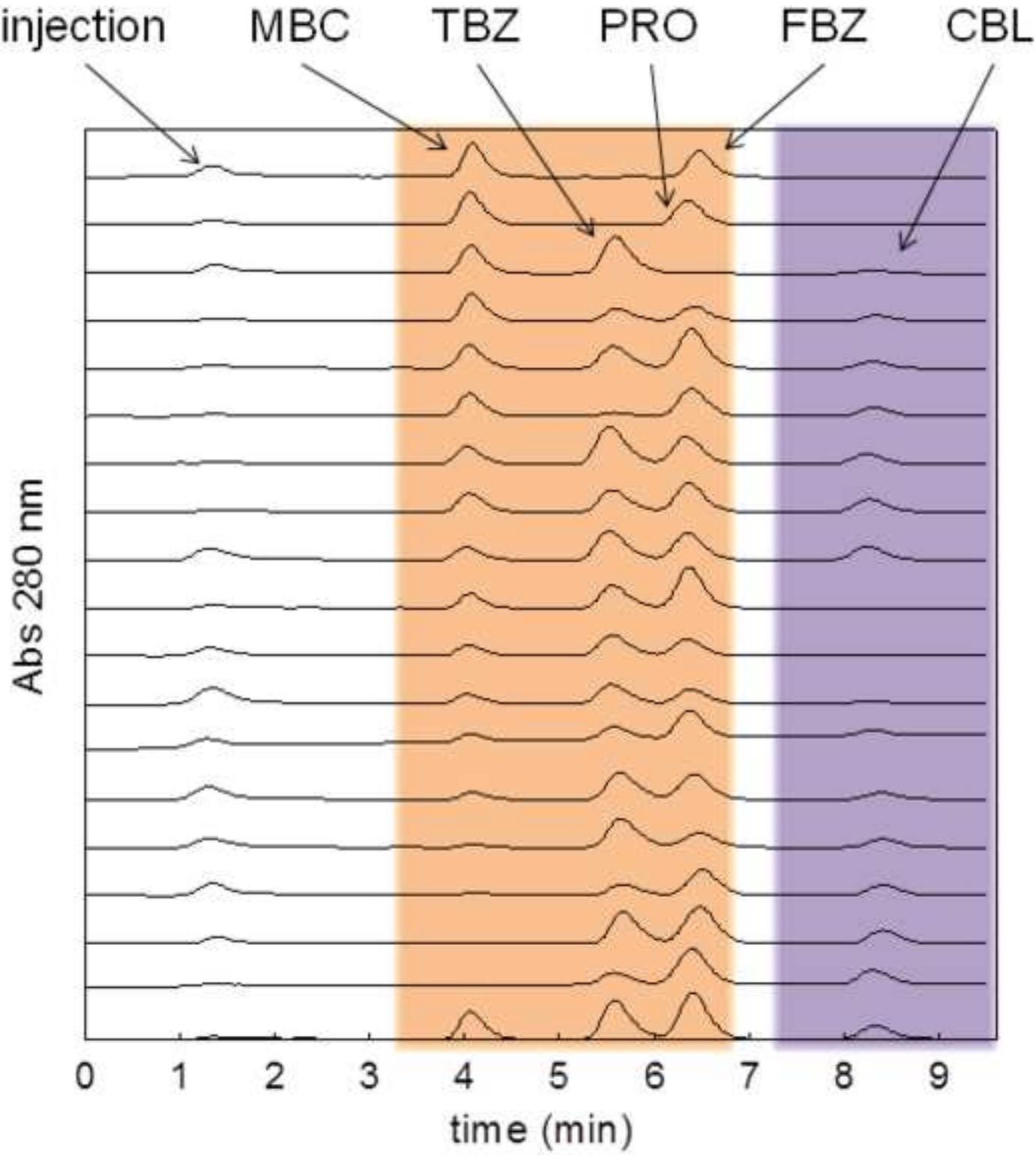

Figure 3

Click here to download high resolution image

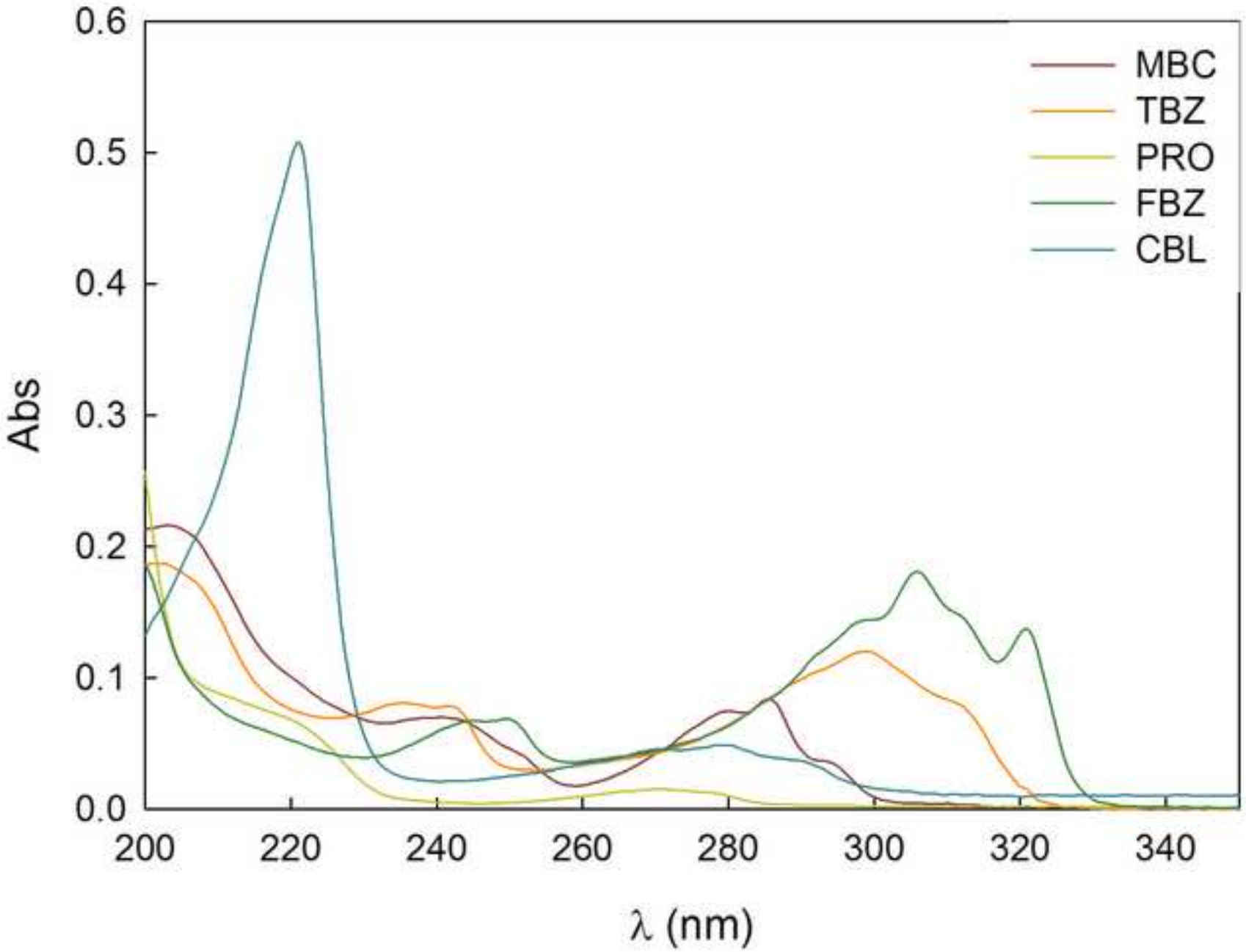

Figure 4

Click here to download high resolution image

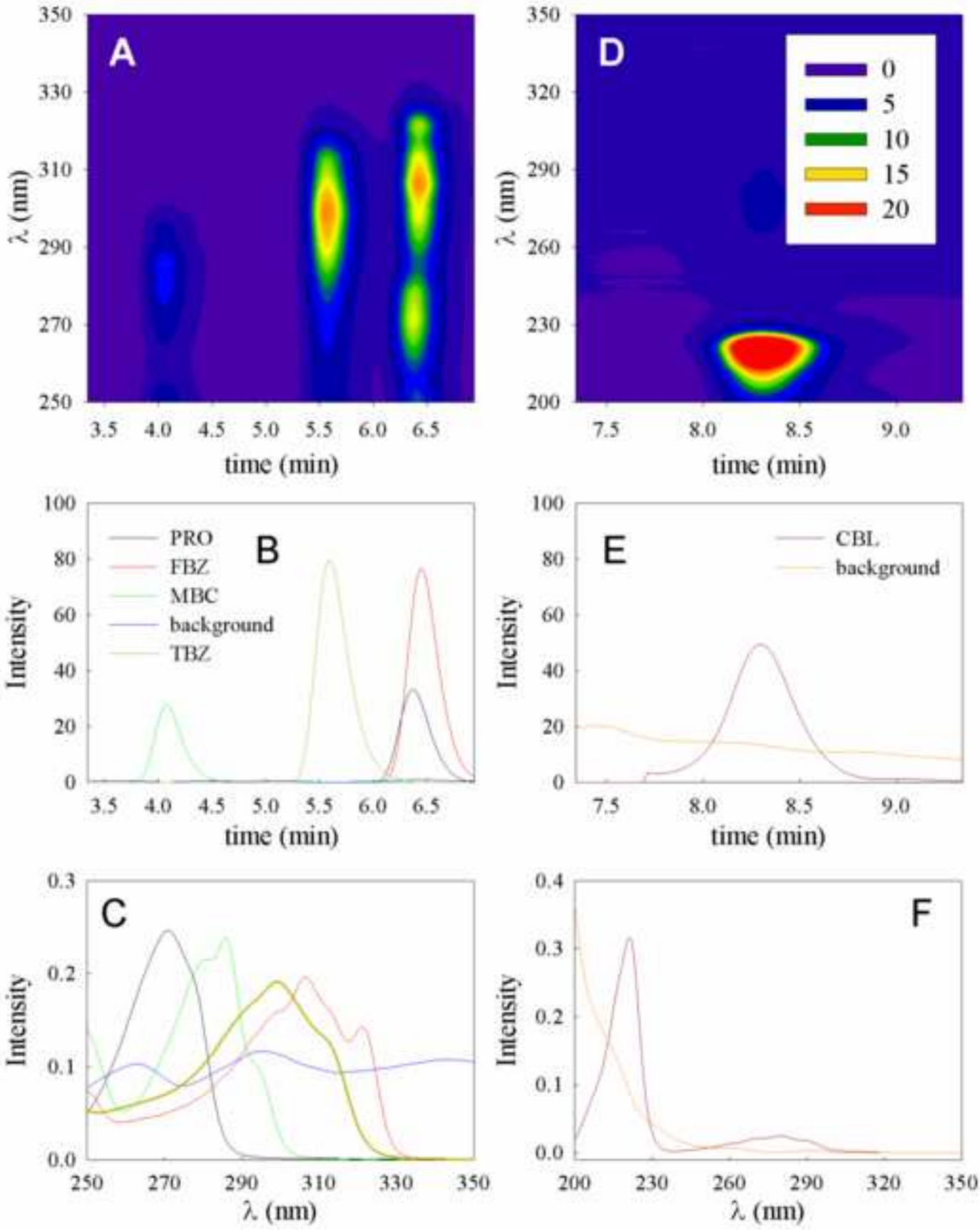

Figure 5

Click here to download high resolution image